

Aus dem Institut für Pädiatrische Endokrinologie  
der Medizinischen Fakultät Charité – Universitätsmedizin Berlin

DISSERTATION

Inactivating *Gnas*-mutations and their impact on the capacity of  
adipose-derived stromal cells to differentiate into adipocytes:  
Implications for the pathogenesis of progressive osseous  
heteroplasia

zur Erlangung des akademischen Grades  
Doctor medicinae (Dr. med.)

vorgelegt der Medizinischen Fakultät  
Charité – Universitätsmedizin Berlin

von

Sinan Akdeniz

aus Berlin

Datum der Promotion: 04.09.2015

# Table of Contents

Table of Contents .....	ii
List of Figures .....	iv
List of Tables .....	vi
List of Abbreviations .....	vii
<b>0 Abstract.....</b>	<b>10</b>
<b>1 Introduction and Hypotheses.....</b>	<b>14</b>
1.1 Progressive osseous heteroplasia (POH).....	14
1.2 Other developmental disorders of heterotopic ossification.....	18
1.2.1 Fibrodysplasia ossificans progressiva (FOP).....	18
1.2.2 Albright hereditary osteodystrophy (AHO).....	20
1.3 The <i>GNAS</i> complex gene and its involvement in POH .....	24
1.4 Hypotheses.....	30
<b>2 Methodology .....</b>	<b>34</b>
2.1 Mouse strains and genotyping .....	34
2.2 Isolation of adipose-derived stromal cells (ADSCs) from mice .....	36
2.3 Cell culture.....	37
2.4 Adipogenic differentiation of ADSCs.....	37
2.5 Total RNA extraction from ADSCs and RNA concentration measurement .....	38
2.6 First-strand cDNA synthesis.....	38
2.7 Real-time quantitative reverse-transcription PCR (qRT-PCR).....	39
2.8 Oil Red O staining .....	39
2.9 Statistical analysis .....	40
<b>3 Results .....</b>	<b>41</b>
3.1 Gene expression measurements.....	41
3.1.1 Expression levels of the alpha-subunit of the stimulatory G protein ( <i>G<math>\alpha</math></i> ) in ADSCs from heterozygous E2KO mice vs. CD1 wt mice.....	41
3.1.2 Expression levels of the extra-large alpha-subunit (XL $\alpha$ s) in ADSCs from .....	43
heterozygous E2KO mice vs. CD1 wt mice.....	43
3.1.3 Expression levels of adipogenic markers in ADSCs from paternal E2KO mice .....	44
vs. CD1 wt mice.....	44
3.1.4 Expression levels of adipogenic markers in ADSCs from maternal E2KO mice.....	50
vs. CD1 wt mice.....	50
3.1.5 Comparison of expression levels of adipogenic markers in ADSCs from CD1 wt mice between experiments .....	54

3.2	Oil Red O results .....	57
3.2.1	Oil Red O elution in ADSCs from paternal E2KO mice vs. CD1 wt mice .....	57
3.2.2	Oil Red O elution in ADSCs from maternal E2KO mice vs. CD1 wt mice .....	60
<b>4</b>	<b>Discussion .....</b>	<b>65</b>
<b>5</b>	<b>Bibliography.....</b>	<b>74</b>
<b>6</b>	<b>Affidavit .....</b>	<b>80</b>
<b>7</b>	<b>Curriculum Vitae .....</b>	<b>81</b>
<b>8</b>	<b>Acknowledgements .....</b>	<b>83</b>

## List of Figures

<b>Figure 1:</b> Histopathology of a POH lesion, manifesting irregular bone deposits within the dermis (hematoxylin/eosin staining). .....	15
<b>Figure 2:</b> Photograph and radiograph of the left upper limb of a patient with POH. ....	16
<b>Figure 3:</b> Clinical and radiographic features of POH in three patients. ....	17
<b>Figure 4:</b> Clinical features of FOP. ....	19
<b>Figure 5:</b> Clinical features of AHO in a 71-year-old female patient. ....	21
<b>Figure 6:</b> Distinct phenotypes of newborn E2KO pups. ....	28
<b>Figure 7:</b> The <i>Gnas</i> complex gene. ....	28
<b>Figure 8:</b> Characteristic double bands for knockout mice as seen after electrophoresis. ...	36
<b>Figure 9:</b> <i>Gsa</i> mRNA expression in ADSCs from CD1 wt vs. pat E2KO mice. (n=5) .....	41
<b>Figure 10:</b> <i>Gsa</i> mRNA expression in ADSCs from CD1 wt vs. mat E2KO mice. (n=4) .....	42
<b>Figure 11:</b> <i>XLas</i> mRNA expression in ADSCs from CD1 wt vs. pat E2KO mice. (n=5) .....	43
<b>Figure 12:</b> <i>XLas</i> mRNA expression in ADSCs from CD1 wt vs. mat E2KO mice. (n=4) ....	44
<b>Figure 13:</b> Absolute <i>PPAR<math>\gamma</math></i> mRNA expression in ADSCs from CD1 wt vs. pat E2KO mice. (n=4).....	45
<b>Figure 14:</b> <i>PPAR<math>\gamma</math></i> mRNA expression in ADSCs from CD1 wt vs. pat E2KO mice each normalized to CD1 wt Day 0. (n=4). ....	47
<b>Figure 15:</b> Absolute <i>aP2</i> mRNA expression in ADSCs from CD1 wt vs. pat E2KO mice. (n=4) .....	48
<b>Figure 16:</b> <i>aP2</i> mRNA expression in ADSCs from CD1 wt vs. pat E2KO mice each normalized to CD1 wt Day 0. (n=4). ....	49
<b>Figure 17:</b> Absolute <i>PPAR<math>\gamma</math></i> mRNA expression in ADSCs from CD1 wt vs. mat E2KO mice. (n=4, except for Day 3 with n=3). ....	50
<b>Figure 18:</b> <i>PPAR<math>\gamma</math></i> mRNA expression in ADSCs from CD1 wt vs. mat E2KO mice each normalized to CD1 wt Day 0. (n=4, except for Day 3 with n=3). ....	51

<b>Figure 19:</b> Absolute aP2 mRNA expression in ADSCs from CD1 wt vs. mat E2KO mice. (n=4, except for Day 3 with n=3). .....	53
<b>Figure 20:</b> aP2 mRNA expression in ADSCs from CD1 wt vs. mat E2KO mice each normalized to CD1 wt Day 0. (n=4, except for Day 3 with n=3). .....	54
<b>Figure 21:</b> Absolute PPAR $\gamma$ mRNA expression in ADSCs from CD1 wt mice. (n=4, except for Day 3 of CD1 wt_Day t (mat E2KO) with n=3) .....	55
<b>Figure 22:</b> Absolute aP2 mRNA expression in ADSCs from CD1 wt mice. (n=4, except for Day 3 of CD1 wt_Day t (mat E2KO) with n=3) .....	56
<b>Figure 23:</b> Relative amounts of Oil Red O in ADSCs from CD1 wt vs. pat E2KO mice normalized to CD1 wt. (n=3). .....	57
<b>Figure 24:</b> Oil Red O staining of CD1 wt and pat E2KO ADSCs on Day 7 of adipogenic differentiation. (experiment #38) .....	58
<b>Figure 25:</b> Oil Red O staining of CD1 wt and pat E2KO ADSCs on Day 7 of adipogenic differentiation. (experiment #43) .....	59
<b>Figure 26:</b> Oil Red O staining of CD1 wt and pat E2KO ADSCs on Day 7 of adipogenic differentiation. (experiment #46) .....	60
<b>Figure 27:</b> Relative amounts of Oil Red O in ADSCs from CD1 wt vs. mat E2KO mice normalized to CD1 wt. (n=3). .....	61
<b>Figure 28:</b> Oil Red O staining of CD1 wt and mat E2KO ADSCs on Day 7 of adipogenic differentiation. (experiment #32) .....	62
<b>Figure 29:</b> Oil Red O staining of CD1 wt and mat E2KO ADSCs on Day 7 of adipogenic differentiation. (experiment #37) .....	63
<b>Figure 30:</b> Oil Red O staining of CD1 wt and mat E2KO ADSCs on Day 7 of adipogenic differentiation. (experiment #47) .....	64

## List of Tables

<b>Table 1:</b> Features of heterotopic ossification in POH, FOP, and AHO. ....	22
<b>Table 2:</b> Clinical, pathological and molecular features of PHP1a, PPHP, and POH. ....	24
<b>Table 3:</b> Genetically manipulated mouse strains used in our studies. ....	32
<b>Table 4:</b> Primer sequences for genotyping of newborn mice. ....	35
<b>Table 5:</b> Primer sequences of different murine genes analysed by qRT-PCR. ....	39

## List of Abbreviations

$\alpha$	-	alpha
$\alpha$ MEM	-	alpha modification of Eagle's medium
ACVR1	-	activin receptor type-1
ADSCs	-	adipose-derived stromal cells
AHO	-	Albright hereditary osteodystrophy
ALK2	-	activin-like kinase-2
aP2	-	adipocyte lipid-binding protein 2
AS	-	antisense transcript
$\beta$	-	beta
BMP	-	bone morphogenetic protein
cAMP	-	cyclic adenosine monophosphate
cDNA	-	complementary DNA
CO <sub>2</sub>	-	carbon dioxide
CPK	-	creatine phosphokinase
ddH <sub>2</sub> O	-	double-distilled water
DMEM	-	Dulbecco's Modified Eagle Medium
DNA	-	deoxyribonucleic acid
E2KO	-	exon 2 knockout
EDTA	-	ethylenediaminetetraacetic acid
EU	-	European Union
FBS	-	fetal bovine serum
Fig.	-	Figure
FOP	-	fibrodysplasia ossificans progressiva
$\gamma$	-	gamma
g	-	gravity
GDP	-	guanosine diphosphate
GFP	-	green fluorescent protein
GPCRs	-	G protein-coupled receptors
G protein	-	guanine nucleotide-binding protein

Gs	-	stimulatory G protein
Gs $\alpha$	-	alpha-subunit of the stimulatory G protein
GTP	-	guanosine triphosphate
i. e.	-	id est
kb	-	kilobase
kDa	-	kilodalton
ko	-	knockout
LDH	-	lactate dehydrogenase
mat	-	maternal
mat E2KO	-	<i>Gnas</i> exon 2 maternal ko
mL	-	milliliter
mM	-	millimolar
mRNA	-	messenger RNA
NaOH	-	sodium hydroxide
NESP55	-	neuroendocrine-specific protein of 55 kDa
nm	-	nanometer
OMIM	-	Online Mendelian Inheritance in Man (registry)
pat	-	paternal
pat E2KO	-	<i>Gnas</i> exon 2 paternal ko
PBS	-	phosphate buffered saline
PCR	-	polymerase chain reaction
POH	-	progressive osseous heteroplasia
PPAR $\gamma$	-	peroxisome proliferator-activated receptor gamma
PTH	-	parathyroid hormone
qRT-PCR	-	quantitative reverse-transcription PCR
RNA	-	ribonucleic acid
s.e.m.	-	standard error of the mean
Tris-HCl	-	tris(hydroxymethyl)aminomethane hydrochloride
TSH	-	thyroid-stimulating hormone
vs.	-	versus
XL $\alpha$ s	-	extra-large alpha-subunit (of the stimulatory G protein)
XLKO	-	<i>Gnasxl</i> ko
$\mu$ g	-	microgram



$\mu\text{L}$  - microliter  
 $\mu\text{m}$  - micrometer

## 0 Abstract

### Introduction

Progressive osseous heteroplasia (POH) is a rare disease of mesenchymal stem cell differentiation leading to heterotopic ossification. It is characterized by ectopic dermal ossifications during infancy that progress from subcutaneous fat tissue into deeper connective tissues during childhood, including tendons, fascia and skeletal muscle. The genetic cause of this disease is a heterozygous inactivation of *GNAS*, which gives rise to a variety of gene products including the alpha-subunit of the stimulatory G protein (*Gsa*) and its extra-large variant XLas.

### Methodology

Since XLas can mimic *Gsa* action, and since *Gsa* deficiency promotes osteogenic fate of stem cells, we hypothesized that XLas deficiency in combination with *Gsa* haploinsufficiency contributes to the development of heterotopic ossifications. The aim of the thesis is to test a preferential osteogenic cell fate of adipose-derived stromal cells (ADSCs) isolated from a POH animal model. Experimental results were obtained from adipogenic differentiation of ADSCs isolated from paternal and maternal *Gnas* exon 2 knockout (E2KO) mice compared to wild-type littermates. ADSCs were differentiated for 12 days and screened for gene expression levels of two adipogenic markers, peroxisome proliferator-activated receptor gamma (PPAR $\gamma$ ) and adipocyte lipid-binding protein (aP2). Moreover, Oil Red O stainings of ADSCs were performed on Day 7 of differentiation to determine intracellular lipid accumulation.

### Results

Results were variable among replicas. However, paternal E2KO cells tended to have higher PPAR $\gamma$  and aP2 mRNA levels before initiation of adipogenic differentiation and to differentiate faster than wild-type cells, although the differences were not statistically significant. Maternal E2KO cells, in contrast, showed similar PPAR $\gamma$  and aP2 expression levels before initiation of adipogenic differentiation and similar adipogenic differentiation profiles to wild-type cells. Oil Red O stains of the cells following seven days of growth under adipogenic conditions appeared to be consistent with increased differentiation of paternal, but not maternal, E2KO ADSCs, although the difference

between the quantified values in wild-type and paternal E2KO cells was not statistically significant.

### **Conclusion**

Our investigation of ADSCs and their genotype-specific capacity for adipogenic differentiation has suggested increased adipogenic potential for ADSCs from paternal E2KO mice and seemingly normal adipogenic potential for maternal E2KO mice compared to wild-type littermates. These findings are opposite of what we originally hypothesized and suggest that XL $\alpha$ s deficiency may increase adipogenic differentiation potential of ADSCs.

## **Abstract**

### **Einleitung**

Progressive osseous heteroplasia (POH; deutsch: progressive knöcherne Heteroplasie) ist eine seltene Krankheit mesenchymaler Stammzell-Differenzierung, welche zu heterotoper Ossifikation führt. Die Krankheit ist gekennzeichnet durch ektopische dermale Ossifikationen während des Säuglingsalters, welche während der Kindheit vom subkutanen Fettgewebe in tiefere Bindegewebsschichten, einschließlich Sehngewebe, Faszien und Skelettmuskel, fortschreiten. Die genetische Ursache dieser Krankheit ist eine heterozygote Inaktivierung von *GNAS*, welches eine Vielfalt von Genprodukten ermöglicht, wie die alpha-Untereinheit des stimulierenden G-Proteins ( $G\alpha$ ) und dessen extra-große Variante XL $\alpha$ s.

### **Methodik**

Da XL $\alpha$ s  $G\alpha$ -Aktion nachahmen kann und  $G\alpha$ -Defizienz ein osteogenes Schicksal von Stammzellen fördert, stellten wir die Hypothese auf, dass XL $\alpha$ s-Defizienz in Kombination mit  $G\alpha$ -Haploinsuffizienz der Entwicklung von heterotopen Ossifikationen beiträgt. Das Ziel der Dissertation ist die Untersuchung eines bevorzugt osteogenetischen Zellschicksals von aus Fettgewebe stammenden Bindegewebszellen (ADSCs, adipose-derived stromal cells), welche aus einem POH-Tiermodell isoliert wurden. Experimentelle Ergebnisse wurden durch adipogenetische Differenzierung von ADSCs erzielt, welche aus paternalen und maternalen *Gnas* exon 2 Knockout-Mäusen (E2KO) isoliert und mit Wildtyp-Wurfgeschwistern verglichen wurden. ADSCs wurden 12 Tage lang differenziert und Genexpressionsraten zweier adipogenetischer Marker, d. h. Peroxisom-Proliferator-aktivierter Rezeptor gamma (PPAR $\gamma$ ) und adipocyte lipid-binding protein (aP2), untersucht. Zudem wurden Oil-Red-O-Färbungen von ADSCs am Tag 7 der Differenzierung durchgeführt, um die intrazelluläre Lipidakkumulation zu bestimmen.

### **Ergebnisse**

Ergebnisse waren variabel unter den Replikaten. Dennoch tendierten die paternalen E2KO-Zellen vor Beginn der adipogenetischen Differenzierung zu höheren PPAR $\gamma$  und aP2 mRNA Raten und differenzierten schneller als Wildtyp-Zellen, wenn auch der

Unterschied nicht statistisch signifikant war. Maternale E2KO-Zellen dagegen zeigten vor Beginn der adipogenetischen Differenzierung ähnliche PPAR $\gamma$  und aP2 Expressionsraten und ähnliche adipogenetische Differenzierungsprofile wie Wildtyp-Zellen. Oil-Red-O- Färbungen der Zellen, welche sieben Tage nach Wachstum unter adipogenetischen Bedingungen folgten, schienen mit einer gesteigerten Differenzierung von paternalen, aber nicht maternalen, E2KO ADSCs übereinstimmend, obwohl der Unterschied zwischen den quantifizierten Werten der Wildtyp- und paternalen E2KO-Zellen nicht statistisch signifikant war.

### **Schlussfolgerung**

Unsere Untersuchung von ADSCs und ihrer genotyp-spezifischen Fähigkeit zur adipogenetischen Differenzierung hat auf ein gesteigertes adipogenetisches Potential für aus paternalen E2KO-Mäusen stammende ADSCs und ein scheinbar normales adipogenetisches Potential für ADSCs aus maternalen E2KO-Mäusen im Vergleich zum Wildtyp hingewiesen. Diese Ergebnisse sind entgegengesetzt zu dem, was wir ursprünglich als Hypothese aufstellten, und suggerieren daher, dass XLas-Defizienz das adipogenetische Differenzierungspotential von ADSCs erhöhen kann.

# 1 Introduction and Hypotheses

## 1.1 Progressive osseous heteroplasia (POH)

Even though many rare diseases show a particularly low prevalence, between 27 million and 36 million people living in the European Union (EU), i. e. 6-8 % of the EU population, suffer from a rare disease.<sup>1-3</sup> In addition, between 5000 and 8000 distinct rare diseases exist today, but exact estimates vary as countries define rare diseases differently.<sup>3,4</sup> The EU defines a rare disease as a life-threatening or chronically debilitating "disease affecting no more than 5 per 10,000 persons in the European Union", though most patients with rare diseases suffer from less frequently occurring diseases affecting 1 in 100,000 people or even fewer patients.<sup>1</sup>

Rare diseases are often neglected diseases and therefore deserve special scientific devotion. Progressive osseous heteroplasia (POH) is such a rare disease of heterotopic ossification. In 1994, POH was first described by Kaplan et al. and in 2000 defined as a *"developmental disorder of mesenchymal differentiation characterized by dermal ossification during infancy and by progressive heterotopic ossification of cutaneous, subcutaneous, and deep connective tissue during childhood"*.<sup>5,6</sup>

Since then, it has received a growing scientific interest, as knowledge and understanding about the pathogenesis involved in POH and other rare disorders have broader implications for a wide variety of more common diseases.

POH (OMIM<sup>i</sup> 166350) is an exceedingly rare autosomal dominant disorder of mesenchymal differentiation and heterotopic ossification caused almost exclusively by paternally inherited inactivating mutations in *GNAS* (formerly *GNAS1*; OMIM 139320), a gene that encodes the alpha-subunit of the stimulatory G protein (G $\alpha$ ) which itself is a signalling protein involved in second messenger cascades.<sup>7,8</sup> However, approximately 30 % of patients with the clinical diagnosis of POH do not possess mutations of *GNAS*.<sup>7,8</sup> Around the world, less than 60 cases of POH have been clinically confirmed.<sup>9</sup> The initial appearance of POH involves the de-novo-formation of bone in reticular

---

<sup>i</sup> Online Mendelian Inheritance in Man (OMIM), a catalogue of human genes and genetic disorders. (<http://www.ncbi.nlm.nih.gov/omim>)

dermis and subcutaneous fat (Fig. 1) through predominantly intramembranous mechanisms, i. e. mesenchymal cells differentiate directly into bone-forming osteoblasts, indicating that the underlying pathology entails a defect in the mesenchymal stem cell fate.<sup>5,6,8,10-12</sup> However, also scarce and limited endochondral ossification, i. e. with prior formation of cartilage, has been observed amidst some of the affected tissues or their contiguous regions as well.<sup>5,6</sup> Within the pathological process of heterotopic ossification osteogenesis occurs in nonskeletal tissues, forming qualitatively normal skeletal bone.<sup>9,13,14</sup>

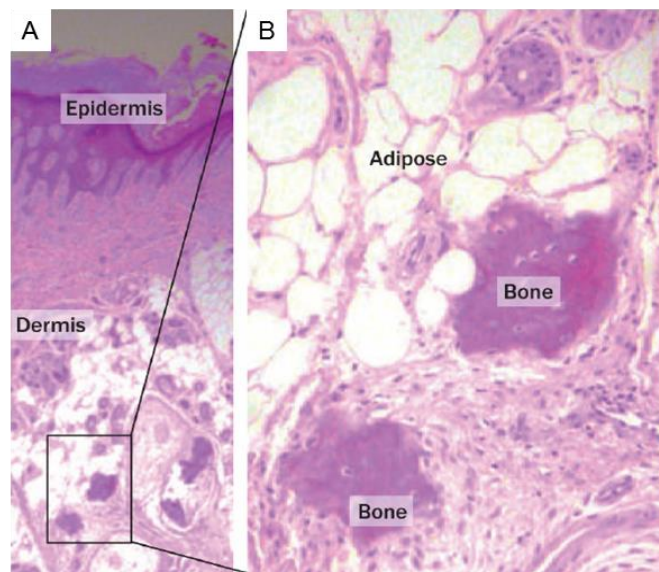


**Figure 1: Histopathology of a POH lesion, manifesting irregular bone deposits within the dermis (hematoxylin/eosin staining).**

(A) 50x amplification. (B) 200x amplification. Abbreviations: POH, progressive osseous heteroplasia. (Adapted from Shore EM and Kaplan FS, 2010)<sup>9</sup>

Primary infantile dermal ossification is accompanied by corresponding areas of congenital maculopapular lesions. Osseous heteroplasia in infancy is a non-inflammatory process and lesions are asymmetrically scattered.<sup>5,6</sup> Typically, radiographs display a diffuse, web-like reticular pattern of POH-type heterotopic ossification (Fig. 2).<sup>15</sup>

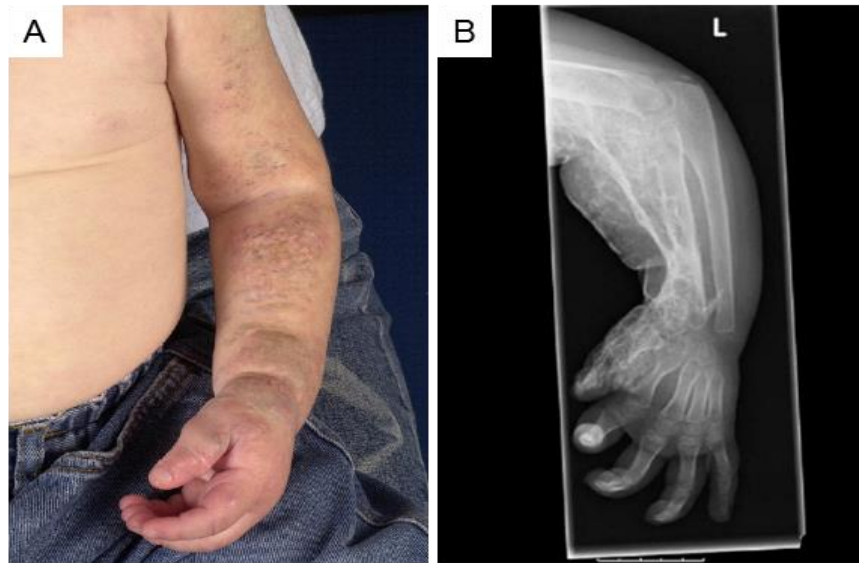


**Figure 2: Photograph and radiograph of the left upper limb of a patient with POH.**

(A) Linear papular pattern of cutaneous heterotopic ossification at 2.5 years of age. (B) Characteristic web-like reticular pattern of POH-type heterotopic ossification in the same patient at 8 years of age, affecting particularly the radial side of the forearm and causing ankylosis of the elbow. Abbreviations: POH, progressive osseous heteroplasia. (Adapted from Schimmel RJ, Pasmans SG, Xu M, et al., 2010)<sup>15</sup>

During childhood islands of heterotopic bone coalesce into plaques.<sup>5,6</sup> As a matter of fact, the disease characteristically manifests by a progression of ectopic bone formation from the skin and subcutaneous tissues into deep connective tissue that include tendons, fascia, skeletal muscle and ligaments, underlying areas of earlier involvement of the skin.<sup>5,6,8,16,17</sup> This heterotopic ossification in extraskeletal soft tissues as well as its progression from superficial to deeper tissue is critical for the distinction of POH.<sup>8,18</sup> The phenotype among patients with POH varies widely in its degree of severity.<sup>7</sup> Ectopic bone formation can lead to a variety of developmental defects and morphological abnormalities in extremities as well as surrounding tissues (Fig. 3). In some individuals, muscles can be largely replaced by heterotopic bone.<sup>5</sup> The extensive ossification of the deep connective tissue can cause ankylosis of affected joints and limbs, resulting in a minimum residual motion. Severe growth retardation and a complete loss of function of affected limbs have also been observed.<sup>5,6,19,20</sup> Furthermore, some patients developed digital anomalies, e.g. secondary hallux valgus deformities. Even though no evidence of a primary neurological or vascular disorder has been adduced in any patient with POH, these disorders can still be associated with heterotopic bone formation. Examined patients demonstrated de facto an adequate intellectual level for their age, with normal cognitive and motor milestones.<sup>5</sup>



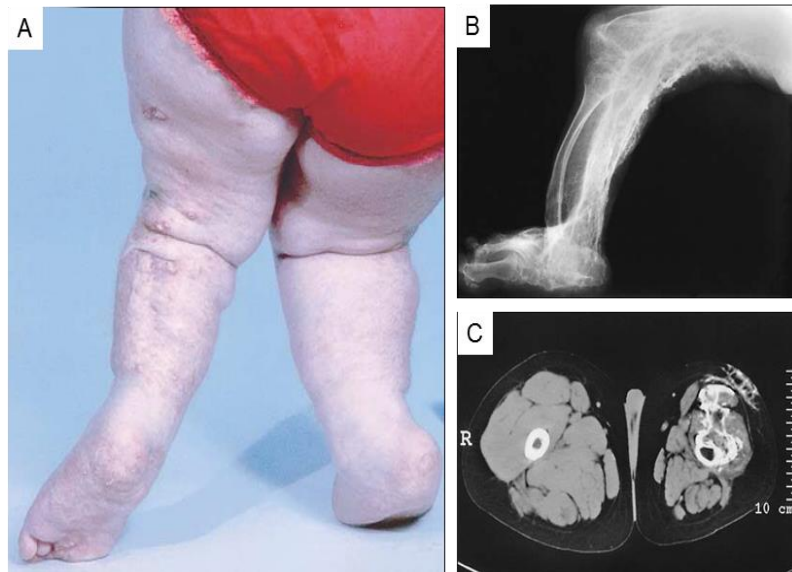


**Figure 3: Clinical and radiographic features of POH in three patients.**

(A) Posterior view of the legs and feet of a five-year-old girl with severe maculopapular lesions, caused by extensive dermal and subcutaneous ossification in the left thigh, leg, foot, and heel. (B) Lateral roentgenogram of the right leg of an 11-year-old girl, showing severe heterotopic ossification of the soft tissues. (C) Computed tomographic image of the thighs of a 10-year-old boy, revealing atrophied soft tissues of the left thigh and extensive soft-tissue ossification of the skin, subcutaneous fat, and quadriceps muscles that extended to the anterior cortex of the femur. Abbreviations: POH, progressive osseous heteroplasia. (Adapted from Shore EM, Ahn J, Jan de Beur S, et al., 2002)<sup>7</sup>

The results of routine laboratory studies among most affected patients with POH have turned out to be normal. Patients with POH have normal endocrine function. Serum levels of calcium, inorganic phosphate, parathyroid hormone (PTH), calcitonin and vitamin D metabolites are unremarkable for most patients. However, elevated levels of serum alkaline phosphatase have been occasionally detected in some individuals during phases of progressive heterotopic osteogenesis.<sup>5,6</sup> Elevated serum levels of lactate dehydrogenase (LDH) and creatine phosphokinase (CPK) have also been observed sporadically, potentially reflecting bone deposition in skin and skeletal muscle.<sup>21</sup>

POH is a devastating, disabling disease that seriously exacerbates the state of health of affected patients. In the last decade, new scientific knowledge has emerged in the field of POH. However, the pathogenesis of this disorder is still not entirely known at present. Besides the possibility of surgically removing well-circumscribed areas of heterotopic

ossification, there is still no effective means of prevention or treatment for POH. The long-term prognosis for patients with POH is yet unclear as only few individuals have been followed beyond adolescence. Yet, it appears in these patients that the progression of the disease followed a slower progression or ceased during adulthood.<sup>5-7</sup> As other rare diseases, POH is probably underdiagnosed. Through the careful investigation of clinical and radiographic features, POH can be distinguished from other rare primary developmental disorders of heterotopic ossification, such as Albright hereditary osteodystrophy (AHO) or fibrodysplasia ossificans progressiva (FOP). Physicians should be aware of the distinctions between these childhood disorders of heterotopic ossification to avoid misdiagnoses and medical malpractice.

## **1.2 Other developmental disorders of heterotopic ossification**

### **1.2.1 Fibrodysplasia ossificans progressiva (FOP)**

Unlike the osteogenesis in POH, the rare and severely debilitating disease fibrodysplasia ossificans progressiva (FOP; OMIM 135100) is characterized by progressive heterotopic ossification formed by predominantly endochondral mechanisms, i. e. mesenchymal cells differentiate into chondrocytes that are gradually replaced by bone containing osteoblasts and osteoclasts.<sup>5,6,10,12</sup> This most disabling condition of ectopic skeletogenesis has a worldwide prevalence of approximately one case in 2 million individuals with more than 700 cases identified.<sup>9,14,22</sup> Most of these FOP cases occur sporadically. However, autosomal dominant inheritance has been observed in a small number of families, with mutations inherited paternally or maternally.<sup>9</sup> FOP has been associated with the 2q23-24 region of chromosome 2.<sup>18,23</sup> In fact, a single heterozygous activating mutation in the glycine-serine activation domain of activin receptor type-1/activin-like kinase-2 (ACVR1/ALK2; OMIM 102576), a bone morphogenetic protein (BMP) type I receptor, was identified in all classically affected individuals, causing a single amino acid substitution of arginine by histidine in codon 206 (c.617G>A; R206H) and provoking dysregulated BMP signalling.<sup>14,23-26</sup> Consequently, this mutation changes the regulation of progenitor cell differentiation.<sup>27</sup> There is no cutaneous and subcutaneous ossification in FOP, but a similarly widespread progressive heterotopic ossification of deep connective tissue as in POH

(Fig. 4B), which forms the first pillar of two major diagnostic characteristics in “classic” FOP.<sup>5,6,18</sup> This extra-skeletal bone formation involves skeletal muscles, tendons, ligaments, fascia as well as aponeuroses, generating a functional bone organ system. It occurs episodically and is accompanied by painful preosseous inflammatory tumor-like swellings (so-called “flare-ups”) that typically occur during the first decade of life and transform into bone.<sup>6,9,14,18,27,28</sup> Heterotopic ossification forms qualitatively normal skeletal bone.<sup>13,14</sup> The second distinct characteristic of FOP is a congenital malformation of the great toes (hallux valgus, malformed first metatarsal, and/or monophalangism; Figure 4A), which is not to be mistaken for a secondary deformity of the great toes as occurring in patients with POH.<sup>5,14,18</sup> At birth, this congenital malformation of the great toes is the only obvious, most recognizable and earliest observation.<sup>9</sup>

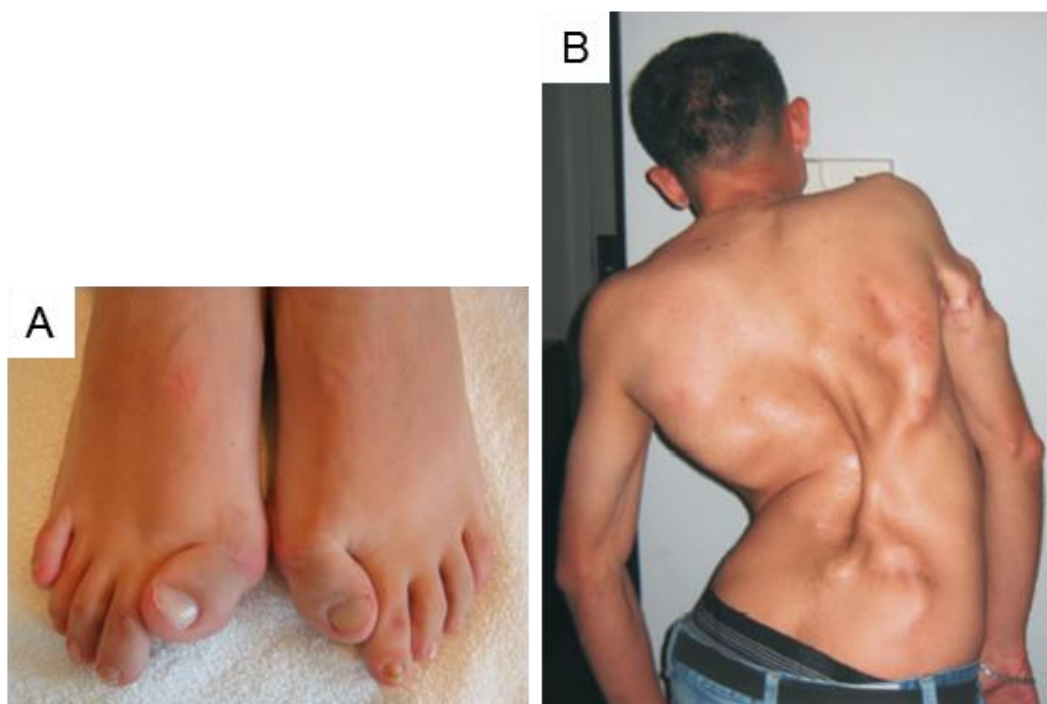


**Figure 4: Clinical features of FOP.**

(A) Characteristic malformation of the great toes. (B) Extensive heterotopic ossification, here protruding from the back and right arm of a patient with FOP and causing considerable deformation. Abbreviations: FOP, fibrodysplasia ossificans progressiva. (Adapted from Pignolo RJ, Shore EM, Kaplan FS, et al., 2011; Kaplan J, Kaplan FS, Shore EM, 2012)<sup>14,25</sup>

The phenotype of FOP includes predictable regional anatomic patterns of distribution (dorsal to ventral, axial to appendicular, cranial to caudal, proximal to distal).<sup>6,18</sup>

Heterotopic bone formation usually starts in the neck and upper back and later episodically progresses to infiltrate the trunk as well as extremities.<sup>27</sup> As a result of extra-skeletal formation and skeletal malformation, further clinical features, including extensive extra-articular ankylosis and scoliosis, may present in patients with FOP, often causing loss of mobility by the second decade of life.<sup>14,29</sup> Moreover, some individuals with FOP present with pneumonia and right-sided heart failure due to thoracic insufficiency syndrome.<sup>14,30</sup> Frequently observed neurological symptoms among FOP patients<sup>22</sup>, such as recurrent severe headache, myoclonus and sensory abnormalities have recently been linked to dysregulated BMP signalling, being responsible for central nervous system demyelination.<sup>31</sup> Surgical removal of heterotopic bone has been experienced to induce explosive new bone growth and should therefore not be undertaken.<sup>14</sup> Other soft tissue injury, such as through preschool immunization, may also elicit exacerbation in patients.<sup>14,28,32</sup> Pharmacotherapy is restricted to treatment of flare-ups that affect major joints, jaw or submandibular area by using high-dose corticosteroids within 24 hours of a new flare-up for a period of four days.<sup>14</sup>

### **1.2.2 Albright hereditary osteodystrophy (AHO)**

Another rare primary developmental disorder of heterotopic ossification in children is Albright hereditary osteodystrophy (AHO), which refers to a variable set of clinical features comprised of brachydactyly / brachymetacarpia, short stature, obesity, subcutaneous ossification or calcification, round face, and often cognitive impairment (Fig. 5).<sup>5,33-36</sup> A high prevalence of carpal tunnel syndrome has often also been identified in patients with AHO.<sup>35</sup>



**Figure 5: Clinical features of AHO in a 71-year-old female patient.**

(A) Absence of the fourth knuckle on each hand and brachymetatarsia of the fourth toes. (B) Radiograph, showing a fourth metacarpal and metatarsal shortening. Abbreviations: AHO, Albright hereditary osteodystrophy. (Adapted from Rolla AR and Rodriguez-Gutierrez R, 2012)<sup>37</sup>

Even though AHO and POH are both associated with intramembranous ossifications in ectopic locations, the lesions in AHO are confined to the skin and superficial tissues only. Frequently, it is therefore also diagnosed as osteoma cutis by dermatologists.<sup>38</sup> AHO shares with POH a more random distribution pattern of heterotopic ossifications and represents another non-inflammatory process of osseous heteroplasia.<sup>5</sup> An overview of features in POH, FOP, and AHO is presented in the table below (Table1).

**Table 1: Features of heterotopic ossification in POH, FOP, and AHO.**

<b>Feature</b>	<b>POH</b>	<b>FOP</b>	<b>AHO</b>
<b>Genetic transmission</b>	Autosomal dominant	Autosomal dominant	Autosomal dominant
<b>Predominant mechanism of ossification</b>	Intramembranous	Endochondral	Intramembranous
<b>Congenital malformation of great toes</b>	-	+	-
<b>Congenital papular rash</b>	+	-	-
<b>Cutaneous ossification</b>	+	-	+/-
<b>Subcutaneous ossification</b>	+	-	+/-
<b>Muscle ossification</b>	+	+	-
<b>Superficial to deep progression of ossification</b>	+	-	-
<b>Severe limitation of mobility</b>	+	+	-
<b>Severe flare-ups of disease</b>	-	+	-
<b>Regional patterns of progression</b>	-	+	-
<b>PTH resistance</b>	- <sup>ii</sup>	-	+/-
<b>Hypocalcemia and hyperphosphatemia</b>	-	-	+/-
<b>Genetic mutations</b>	Heterozygous inactivating mutations of the paternal allele of <i>GNAS</i>	Activating mutation of <i>ACVR1/ALK2</i>	Heterozygous inactivating mutations in <i>GNAS</i>

Abbreviations: POH, progressive osseous heteroplasia; FOP, fibrodysplasia ossificans progressiva; AHO, Albright hereditary osteodystrophy; PTH, parathyroid hormone; *ACVR1/ALK2*, activin receptor type-1/activin-like kinase-2. (Adapted from Kaplan FS and Shore EM, 2000; Schimmel RJ, Pasmans SG, Xu M, et al., 2010)<sup>6,15</sup>

AHO is an autosomal dominant disorder, which in most cases is caused by heterozygous inactivating mutations in *GNAS*, causing an approximately 50 %

<sup>ii</sup> There have been several reports of POH showing evidence of PTH resistance. Those cases presented with hypocalcemia and hyperphosphatemia. Mutations were located on the maternal *GNAS* allele in those cases.

deficiency in  $G\alpha$  expression in most tissues and resulting in  $G\alpha$  haploinsufficiency.<sup>6,7,34,39-41</sup> Phenotypic features of patients with AHO vary considerably, depending on the parent-of-origin of the mutated allele.

Maternal inheritance of *GNAS* mutations is associated with a disorder of multihormone resistance, termed pseudohypoparathyroidism type Ia (PHPIa; OMIM 103580), which primarily involves an end-organ resistance to the actions of the parathyroid hormone (PTH), thyroid-stimulating hormone (TSH), gonadotropins and growth hormone-releasing hormone in the presence of AHO features, particularly obesity.<sup>7,42,43</sup> Mutations occur throughout the entire gene.<sup>39</sup> All of these hormones exert their actions by binding receptors that couple  $G\alpha$  to stimulate adenylyl cyclase.<sup>7,42,43</sup> However, not all hormones or molecules that act via  $G\alpha$  are affected in these patients. For example, while PTH resistance is commonly observed, vasopressin actions appear to be unimpaired.<sup>44</sup> Typically, patients with pseudohypoparathyroidism present with elevated plasma PTH levels in the presence of hypocalcemia and hyperphosphatemia.<sup>39,45</sup> Hypoparathyroidism itself is caused by a lack of PTH rather than by resistance to it, causing likewise hypocalcemia and hyperphosphatemia.<sup>45</sup>

On the contrary, paternal inheritance of *GNAS* mutations results in AHO without multihormone resistance. This disorder is termed pseudopseudohypoparathyroidism (PPHP; OMIM 612463).<sup>7,46</sup> However, patients with paternal *GNAS* mutations mostly lack obesity and cognitive impairment.<sup>33,47</sup> Reports of patients with AHO showing atypically extensive, POH-like heterotopic ossification suggested a common genetic background for the two disorders.<sup>6,48</sup> The following table compares the different features of PHPIa, PPHP, and POH (Table 2). Variable phenotypic expression of AHO and resistance to some, but not all, hormones suggested a tissue-specific manner of imprinting of *GNAS*, with  $G\alpha$  being primarily expressed from the maternal allele in certain hormone-responsive tissues.<sup>44,49,50</sup> Genomic imprinting itself refers to an epigenetic phenomenon that affects a small number of genes, such as *GNAS*, leading to differential gene expression from the two parental alleles with partial or total loss of expression of one allele.<sup>51-53</sup>

**Table 2: Clinical, pathological and molecular features of PHPIa, PPHP, and POH.**

Feature	PHPIa	PPHP	POH
PTH resistance	+	-	-
AHO features	+	+	rarely
Cutaneous and subcutaneous heterotopic ossification	+	+	+
Heterotopic ossification in skeletal muscle and deep connective tissue	-	-	+
Heterozygous loss of function or expression of Gs $\alpha$	+	+	+
GNAS defect	mutations in exons 1-13	mutations in exons 1-13	mutations in exons 1-13
Transmission	maternal	paternal	paternal

Abbreviations: PHPIa, pseudohypoparathyroidism type Ia; PPHP, pseudopseudohypoparathyroidism; POH, progressive osseous heteroplasia; PTH, parathyroid hormone; AHO, Albright hereditary osteodystrophy; Gs $\alpha$ , alpha-subunit of the stimulatory G protein. (Adapted from Kaplan FS and Shore EM, 2000; Izzi B, Francois I, Labarque V, et al., 2012)<sup>6,54</sup>

### 1.3 The *GNAS* complex gene and its involvement in POH

Guanine nucleotide-binding proteins (G proteins) belong to a ubiquitous superfamily of proteins that are capable of binding guanine nucleotides with a high affinity and specificity.<sup>55</sup> Each heterotrimeric G protein is defined by its alpha-subunit, which exchanges guanosine diphosphate (GDP) for guanosine triphosphate (GTP) upon receptor activation thereby allowing dissociation from the  $\beta\gamma$ -complex. Through an intrinsic guanosine triphosphatase activity, the free, active GTP-bound Gs $\alpha$  returns to its GDP-bound state.<sup>7,55-59</sup> One of the most important functions of G proteins is the regulation of signal transduction of extracellular signals from seven-transmembrane / heptahelical receptors (GPCRs, guanine nucleotide-binding protein-coupled receptors) to intracellular effectors, involving the generation of intracellular second messengers,



such as cyclic adenosine monophosphate (cAMP). Moreover, a wide range of extracellular first messengers, including hormones and neurotransmitters, require G proteins for the regulation of cellular activity or function.<sup>7,55-58</sup>

*GNAS* (OMIM 139320), a complex gene located at 20q13.2-13.3 consisting of 13 exons, and its mouse ortholog *Gnas* at distal chromosome 2 consisting of 12 exons encode a variety of gene products.<sup>6,8,60,61</sup> Both human *GNAS* and the murine ortholog *Gnas* exhibit a similar organization and imprinting pattern.<sup>62,63</sup> It is a complex locus, as *GNAS* generates oppositely imprinted gene products, i. e. paternal, maternal, or biallelic transcripts that use alternative promoters and first exons.<sup>34,42,49,56,62</sup> Among these gene products is the alpha-subunit of the stimulatory G protein ( $G\alpha$ ) of adenylyl cyclase, a signalling protein involved in second messenger cascades by increasing levels of cAMP.<sup>6,8,61</sup>  $G\alpha$  signalling is crucial for the formation of normal bone in early osteoblast lineage.<sup>64</sup> Furthermore,  $G\alpha$  plays a distinguished role in regulating the bipotential osteogenic-adipogenic lineage cell fate of mesenchymal progenitor cells in soft tissues.<sup>65-67</sup> It is a ubiquitous protein that is biallelically expressed in most tissues, thus being equally expressed from the paternal and maternal chromosomes.<sup>42,50,63,68</sup> However, in certain tissues, such as in renal proximal tubules (the major site of renal PTH action), thyroid, pituitary, paraventricular nucleus of the hypothalamus, testis, ovary, as well as neonatal murine brown adipose tissue,  $G\alpha$  is predominantly expressed from the maternal allele and paternally silenced, indicating that this monoallelic, parent-of-origin specific  $G\alpha$  expression is imprinted in a tissue-specific manner.<sup>44,63,69-74</sup> This seems to be important in the development of hormone resistance. In fact, in certain hormone targets with a predominantly maternal-specific expression of  $G\alpha$ , mutations on the maternal allele of *GNAS* elicit a considerable decrease in  $G\alpha$  expression and/or activity, being consistent with hormone resistance within the scope of PHPla.<sup>39,63</sup> In contrast, the absence of resistance to multiple hormones, such as TSH, is characteristic in patients with paternal  $G\alpha$  mutations. Thus, mutations in the inactive paternal allele have marginal effects on  $G\alpha$  expression in these tissues affected by imprinting.<sup>70</sup> Disruption of maternal or paternal *Gnas* allele leads to subcutaneous calcified tumor formation in mice, being most likely the result of  $G\alpha$  haploinsufficiency rather than total  $G\alpha$  deficiency.<sup>75</sup>

Alternative promoters and first exons that splice onto common exons 2-13 result in multiple other sense and antisense gene products, such as the extra-large alpha-

subunit (XLas), a variant of Gs $\alpha$ . Both Gs $\alpha$  and XLas utilize exons 2-13, but XLas uses a unique, alternative first exon (exon XL) and a distinct upstream promoter that is active exclusively on the paternal allele.<sup>56,63,76-78</sup> Mutations in patients with POH have been detected almost exclusively on the paternal *GNAS* allele and are located throughout the entire gene in exons 1 through 13, thus mostly affecting both XLas and Gs $\alpha$ , and causing a complete loss of XLas, due to exclusive paternal expression of XLas, and a loss of one Gs $\alpha$  allele.<sup>7,8,11,54,79-81</sup>

XLas has been shown to be associated with the plasma membrane of primarily neuroendocrine tissues, particularly pituitary, and can be additionally detected in cerebellum, pancreas, heart, kidney as well as white and brown adipose tissue.<sup>59,77,82</sup> A recent study has demonstrated that the XLas promoter is also active in the vascular smooth muscle.<sup>83</sup> Furthermore, XLas is expressed in several other cells, including murine bone marrow stromal cells, chondrocytes, calvarial osteoblasts, and human mesenchymal stem cells.<sup>84,85</sup> Studies indicate an interaction of XLas with the  $\beta$  dimer.<sup>86</sup> In fact, sharing most exons, Gs $\alpha$  and XLas exhibit partly identical structural and functional features, which allow XLas to mimic some of the functions of Gs $\alpha$ , such as stimulating cyclic AMP formation in response to different receptor agonists.<sup>76,86-88</sup> Moreover, experiments with *Gnasxl* knockout (XLKO) mice, in which the paternal XLas allele is disrupted, assign to this protein a regulatory function in postnatal feeding, including energy homeostasis and glucose metabolism. In fact, XLas knockout mice demonstrate a failure to adapt to feeding after birth, showing hypoglycaemia and thin bodies and dying mostly within a few days after birth, and thus develop hypoglycaemia and reduced fat mass.<sup>82,89</sup> When they succeed to survive, adult *Gnasxl* mice present with increased glucose tolerance and insulin sensitivity, while being hypermetabolic with reduced fat mass and hypolipidemia.<sup>82</sup> Therefore, a role as a negative regulator of sympathetic nervous system activity in mice has been additionally assigned to XLas.<sup>51,89</sup>

However, a disparity among phenotypes of *Gnasxl* knockout mice<sup>82,89</sup> as opposed to the phenotypes of Gs $\alpha$ -specific exon 1 knockout mice<sup>72,90</sup>, in which Gs $\alpha$ , but not XLas is disrupted, and mice with heterozygous disruption of *Gnas* exon 2<sup>44,91-93</sup>, affecting both Gs $\alpha$  and XLas, indicates non-identical functions of both proteins and assigns a unique role to XLas.

Depending on the parent-of-origin of the disrupted allele, heterozygous disruption of *Gnas* exon 2 causes opposing effects on energy and glucose metabolism as *Gsα* is imprinted in a tissue-specific manner: Paternal E2KO mice are severely lean, showing reduced lipid accumulation in white and brown adipose tissue (Fig. 6). They are hypermetabolic and hyperactive, mostly dying within some hours after birth due to failure to suckle.<sup>44,91-93</sup> Increased sympathetic nervous system activity, glucose tolerance as well as insulin sensitivity in paternal E2KO mice is likely to be a result of *XLαs* deficiency.<sup>89</sup> Paternal *Gsα*-specific exon 1 knockout mice present with mild obesity and minimal glucose intolerance as well as mild insulin resistance.<sup>72,90</sup>

By contrast, maternal E2KO mice have subcutaneous edema at birth, develop obesity with increased lipid accumulation in white and brown adipose tissue and are hypometabolic as well as hypoactive (Fig. 6).<sup>44,92,93</sup> Obesity is also a cardinal feature in maternal *Gsα*-specific exon 1 knockout mice.<sup>72,90</sup> Furthermore, maternal *Gsα*-specific exon 1 knockout mice – unlike maternal E2KO mice – develop glucose intolerance, insulin resistance, and hyperlipidemia.<sup>72,90,94,95</sup> Recently, tissue-specific *Gsα* imprinting was referred to as a requirement for the metabolic consequences of maternal *Gsα* mutations, with obesity resulting from *Gsα* deficiency in one or more metabolically active tissues.<sup>51,96</sup> In fact, obesity has been shown in mice with a maternal, but not paternal, central nervous system-specific *Gsα* deletion.<sup>69</sup> Thus, obesity was associated with imprinting in the central nervous system and a subsequent stimulation defect of the sympathetic nervous system activity and energy expenditure through central melanocortins.<sup>51,69,96</sup> In particular, Chen et al. have shown that *Gsα* is predominantly expressed from the maternal allele in the paraventricular nucleus of the hypothalamus, thereby contributing to obesity.<sup>97</sup>

Homozygous *Gs* deficiency results in embryonic lethality, indicating that the gene is indispensable for normal development.<sup>42,44,65,92</sup>

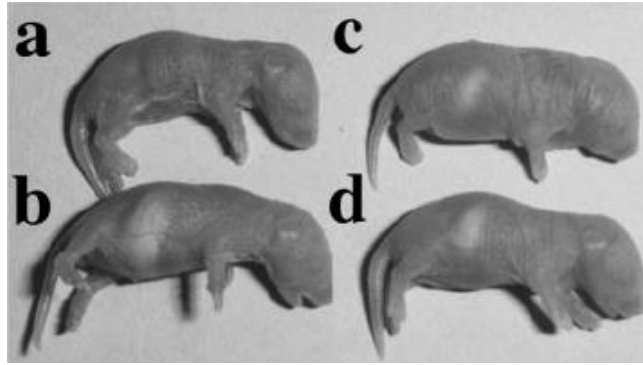


**Figure 6: Distinct phenotypes of newborn E2KO pups.**

(a) paternal E2KO, (c) maternal E2KO, (b) / (d) wild-type littermates. Abbreviation: E2KO, exon 2 knockout.

(Adapted from Yu S, Yu D, Lee E, et al., 1998)<sup>44</sup>

Further major *GNAS* transcripts are generated from alternative transcript-specific promoters and first exons that are spliced to exons 2 through 13, leading to additional oppositely imprinted gene products: the exclusively maternally expressed neuroendocrine-specific protein of 55 kDa (NESP55; Nesp55 in mice) and the exclusively paternally expressed, presumably non-coding A/B transcript (also referred to as 1A or 1'; exon 1A in mice; Figure 7).<sup>7,49,50,63,72,78,98-100</sup> Moreover, another non-coding transcript that is antisense to NESP55 is paternally derived from *GNAS*, called antisense transcript (AS; Nespas in mice).<sup>49,63,100,101</sup> Various *GNAS* products undergo alternative pre-messenger ribonucleic acid (pre-mRNA) splicing, leading to further different variants.<sup>63</sup>

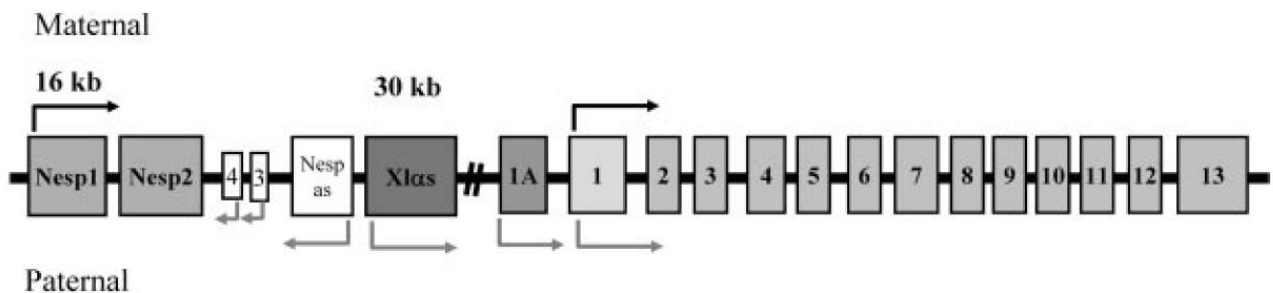


**Figure 7: The *Gnas* complex gene.**  $G\alpha$  is encoded by exons 1 through 13. Three alternative exons upstream of exon 1 are spliced to exons 2 through 13 to produce the exclusively maternally expressed protein Nesp55 (black arrows) as well as  $\alpha$ Ls and exon 1A that are transcribed exclusively from the paternal allele (gray arrows). Abbreviation: kb, kilobase; Nesp55, neuroendocrine-specific protein of 55 kDa;  $\alpha$ Ls, extra-large alpha-subunit (of the stimulatory G protein). (Adapted from Germain-Lee EL, Schwindinger W, Crane JL, et al., 2005)<sup>72</sup>

A wide spectrum of human diseases is caused by G protein disorders.<sup>7,55</sup> As a key regulator of osteoblastic commitment in nonosteogenic connective tissues, *GNAS* usually limits ossification to the skeleton. Therefore, somatic or germ-line mutations in *GNAS* form the basis for numerous bone disorders.<sup>7</sup> Studies on G $\alpha$  and its involvement in mesenchymal stem cell fate uncovered potential inhibitory roles in early osteogenic lineage commitment in nonosseous connective tissues by G $\alpha$  activity and the cyclic AMP signalling pathway, respectively.<sup>102</sup> Hence, such inactivating mutations in *GNAS* could plausibly result in down-regulation of adenylyl cyclase catalyzed pathways, subsequently impair regulation of cyclic AMP-mediated signal transduction in mesenchymal stem cells and inappropriately recruit to an osteogenic lineage from pluripotent mesenchymal cells.<sup>6,40,41,57</sup> While these germ-line inactivating *GNAS* mutations can cause either AHO or POH, somatic activating mutations of *GNAS* with an up-regulation of G $\alpha$  and constitutive (hormone-independent) activation of adenylyl cyclase can result in endocrine tumours or McCune-Albright Syndrome (OMIM 174800).<sup>6-8,55,103</sup> The latter, named by their discoverers McCune and Albright, typically presents with a clinical triad, consisting of hyperpigmented skin lesions (café-au-lait spots), gonadotropin-independent sexual precocity, and fibrous dysplasia of bone, which is a focal and benign fibrous bone lesion.<sup>34,42,48,103</sup> At present, 189 unique DNA variants and 511 individuals with variants have been reported with *GNAS* complex locus.<sup>iii</sup> The cellular role of XL $\alpha$ s is still not obvious and its potential involvement in the regulation of stem cell fate and the pathogenesis of POH remains largely elusive.

Although both bone disorders, AHO and POH, are caused by haploinsufficiency of *GNAS*, one can distinguish POH from AHO and other *GNAS*-based disorders of heterotopic ossification. In fact, ossifications in patients with AHO - as opposed to patients with POH - are limited to the skin and superficial tissues only while POH manifests superficial heterotopic ossification that progresses to deeper tissues in the absence of AHO features and without hormone resistance.<sup>5,7,8</sup> POH therefore appears to be an extreme form of AHO. Why some patients manifest superficial ectopic ossification and others develop POH-like features still needs to be clarified. Albeit

---

<sup>iii</sup> <http://www.ncbi.nlm.nih.gov/omim>; Retrieved 18th July 2014.

unknown, genetic background, environmental factors or epigenetic modifications might account for the invasive nature of ossifications observed in patients with POH.

AHO and isolated POH also show a clear difference in the parental origin of the mutant *GNAS* allele, consistent with the potential involvement of the deficiency of an imprinted *GNAS* gene product.<sup>49,50</sup> Mutations that lead to isolated POH always correlate with a paternal inheritance of the *GNAS* mutation or occur de novo on the paternal *GNAS* allele, suggesting that a paternally derived *GNAS* product regulates progressive osteogenic differentiation and/or proliferation of cells in soft connective tissues.<sup>7</sup> However, it is still not obvious, why in some patients a paternal inheritance of the mutated *GNAS* allele resulted in a less severe manifestation of AHO featuring a lack of hormone resistance (pseudopseudohypoparathyroidism). POH might only depict the end stage of a series of bone disorders caused by *GNAS*.<sup>6</sup> By contrast, maternal inheritance of the mutant *GNAS* allele is associated with AHO and hormone resistance, referred to as pseudohypoparathyroidism type Ia.<sup>7,43</sup>

## 1.4 Hypotheses

A growing number of scientific investigations indicate that multipotent stem cells from adipose tissue can differentiate along an osteogenic and adipogenic lineage<sup>65,104-106</sup> and that *Gsα* may be a key regulator between adipogenesis and osteogenesis<sup>65,104</sup>. Studies by Pignolo et al. revealed accelerated osteoblast differentiation with enhanced expression of osteogenic markers in adipocyte soft tissue stromal cells from paternally inherited *Gsα*-specific exon 1 knockout mice as compared to the same cells isolated from wild-type mice.<sup>104</sup> In a different study, it has also been shown that paternal ablation of *Gsα* exon 1 leads to impaired adipogenic differentiation of stromal cells derived from adipose tissue.<sup>65</sup>

The subcutaneous adipose tissue is of high interest with regard to the pathogenesis of progressive osseous heteroplasia (POH), as it manifests the primary appearance of bone lesions and potentially harbours early dysfunction in signalling pathways. Extraskelatal bone formation requires precursor cells that can potentially differentiate

into bone. ADSCs represent multipotent cells that can lead to ectopic bone formation and/or adipocyte formation in POH.

This thesis will focus on questions with regard to differences in the differentiation capacity of adipose-derived stromal cells (ADSCs) between paternal exon 2 knockout (pat E2KO) and CD1 wt mice as well as between maternal exon 2 knockout (mat E2KO) and CD1 wt mice, respectively (Table 3).

Inactivating mutations causing POH are nearly always paternally inherited and affect common exons of *Gsa* and *XLas*, causing a disruption of one copy of *Gsa* and a complete loss of *XLas*. Our first mouse model thus comprises paternal E2KO mice (Table 3). Paternal E2KO mice are severely lean, demonstrating reduced lipid accumulation in white and brown adipose tissue.<sup>44,91-93</sup> We therefore hypothesize that *XLas* deficiency combined with *Gsa* haploinsufficiency impairs adipogenic lineage commitment of mesenchymal cells more readily than *Gsa* haploinsufficiency alone by further lowering the cAMP levels that are already reduced as a result of *Gsa* haploinsufficiency. And, therefore, as a consequence of this diminished adipogenesis, the mesenchymal cells undergo osteogenesis more readily, thus contributing to the pathogenesis of POH. Paternal E2KO mice will be compared to maternal E2KO mice which lack one copy of *Gsa* only (Table 3). This hypothesis is based on the functional role of *XLas* as a *Gsa*-like protein. *XLas* acts as a potent stimulator of cAMP signalling, which itself is presumed to have a suppressive effect on early stages of osteogenic differentiation and plays opposing roles in osteogenesis vs. adipogenesis.<sup>106-108</sup> Within the scope of this reciprocal relationship cAMP signalling is presumed to thus promote adipogenic differentiation.<sup>106</sup>

The knockout of *Gnas* exon 2 has been previously utilized in a similar model to address the role of *XLas* deficiency in addition to *Gsa* haploinsufficiency in the growth plate. Investigating the differentiation of growth plate chondrocytes in chimeric mice containing both wild-type cells and cells with a heterozygous disruption of the maternal or paternal allele of *Gnas* exon 2, Bastepe et al. have shown that chondrocytes with a paternal *Gnas* exon 2 disruption underwent premature hypertrophy more significantly than those with a maternal *Gnas* exon 2 disruption.<sup>84</sup> Thus, *XLas* deficiency exacerbates the phenotype caused by *Gsa* haploinsufficiency in this setting, similar to our hypothesis

regarding the role of combined XLas deficiency and Gsα haploinsufficiency in the pathogenesis of POH.

In order to test our hypothesis, our research project comprised the investigation of adipose-derived stromal cells derived from *Gnas* exon 2 knockout mice for their lineage commitment and capacity to differentiate into adipocytes. Comparing cells from paternal and maternal *Gnas* exon 2 knockout mice would allow us to determine whether the loss of XLas in addition to the loss of one Gsα allele significantly decreases adipose transformation of these cells. We investigated 1) *Gnas* exon 2 paternal knockout mice, which lack both XLas and one copy of Gsα, and 2) *Gnas* exon 2 maternal knockout mice, which lack one copy of Gsα only (Table 3). *Gnas* exon 2 paternal knockout mice serve as a model for patients with POH.

**Table 3: Genetically manipulated mouse strains used in our studies.**

<b>Mouse strain</b>	<b>Gsα</b> (biallelic expression)	<b>XLas</b> (only paternal expression)
<b><i>Gnas</i> exon 2 ko pat</b>	+/-	-
<b><i>Gnas</i> exon 2 ko mat</b>	+/-	+

Abbreviations: ko, knockout; pat, paternal; mat, maternal.

Adipogenic differentiation was assessed by the expression of adipogenic markers, including peroxisome proliferator-activated receptor (PPAR $\gamma$ ) and adipocyte lipid-binding protein (aP2). Furthermore, Oil Red O stainings were applied to some cell cultures to assess the extent of fat accumulation.

Anticipated results of our study were as follows:

If XLas deficiency does not add to Gsα deficiency, we expected no differences between paternal and maternal *Gnas* exon 2 knockout mice. In contrast, if XLas deficiency adds to Gsα deficiency, cells from paternal *Gnas* exon 2 ko mice were predicted to differentiate into adipocytes less rapidly than those from maternal *Gnas* exon 2 ko mice. Based on the reciprocal relationship between adipogenic and osteogenic differentiation, the latter finding would suggest that XLas deficiency could have a role in ectopic bone formation.



We have developed our hypothesis during the year of 2010, prior to the research visit in Boston. In 2011, at the time when the experiments were conducted, other research groups have worked on very similar working hypotheses however using different mouse models<sup>65,104</sup> (see discussion).

Due to the extent of our research project, this thesis focussed on questions with regard to differences in the adipogenic differentiation capacity of ADSCs between paternal E2KO and CD1 wt as well as between maternal E2KO and CD1 wt, respectively. Therefore, this thesis is to be seen as part of a more complex and larger research project that in other parts aimed to test the further questions of osteogenic differentiation.

## 2 Methodology

My research responsibilities within our research project comprised the genotyping of newborn mice litters and the isolation, cultivation and differentiation of ADSCs from newborn paternal and maternal exon 2 knockout mice as well as from their wild-type littermates. Furthermore, I was responsible for the isolation of cell ribonucleic acid (RNA) on different time points, complementary deoxyribonucleic acid (cDNA) synthesis, quantitative reverse-transcription polymerase chain reaction (qRT-PCR) and the analyses of gene expression levels relative to the expression level of beta-actin. In addition, I have performed all Oil Red O stainings and done the quantitation of Oil Red O elution for all experiments as well as their analyses.

### 2.1 Mouse strains and genotyping

The different mouse strains, i. e. paternal *Gnas* exon 2 ko (pat E2KO) and maternal *Gnas* exon 2 ko (mat E2KO), were available in Dr. Bastepe's laboratory and had been previously generated by targeted mutagenesis.<sup>44,82</sup> Mice were maintained on a 12-h light/dark cycle (6 am/6 pm) and on a standard pellet diet (NIH-07, 5 % fat by weight). Female CD1 wt mice were mated with male heterozygotes and male CD1 wt mice were mated with female heterozygotes to create paternal and maternal E2KO mice, respectively, as previously described.<sup>44</sup>

Animal experiments were approved by and performed in accordance with the standards of the Institutional Animal Care and Use Committee (IACUC), Massachusetts General Hospital, Boston, USA.

Prior to our experiments, newborn litters from crossed adult mice were genotyped with the help of established laboratory protocols:

A small piece of tail tip was obtained from every pup, placed in a 75  $\mu$ L suspension of Alkaline Lysis Reagent with a final concentration of 25 mM sodium hydroxide (NaOH) and 0.2mM ethylenediaminetetraacetic acid (EDTA) and heated up to 95°C for 30 minutes. Thereafter, the suspension was cooled down to 4°C. Another aliquot of 75  $\mu$ L of Neutralization Buffer consisting of a final concentration of 40 mM tris hydroxymethyl

aminomethane-hydrochloride (Tris-HCl) was afterwards added and the whole suspension carefully shaken. PCR could then be performed for each of the genomic DNA samples, by using GoTaq<sup>®</sup> Green Master Mix (Promega), double-distilled water (ddH<sub>2</sub>O) and specific primers (Table 4). Wild-type DNA samples and DNA from knockout mice were used as negative and positive controls, respectively.

**Table 4: Primer sequences for genotyping of newborn mice.**

Genotype		Primer name	Primer sequences
E2KO	beta-globin gene	bGlo-x54	5' CCACAGATCCTATTGCCATGCCC 3'
		bGlo-x56	5' CATAAGACCCCAGTAATGAGCC 3'
	Neomycin-specific primers	Neo-F	5' GATCGGCCATTGAACAAGATG 3'
		Neo-R	5' AAGGTGAGATGACAGGAGATC 3'

Finally, the amplified DNA material was run on a 1.6 % agarose gel by electrophoresis, and the genotypes were subsequently evaluated. Products from knockout mice were identified by double bands, while wild-type littermates showed a single band showing the amplicon from the endogenous beta-globin locus (Fig. 8).

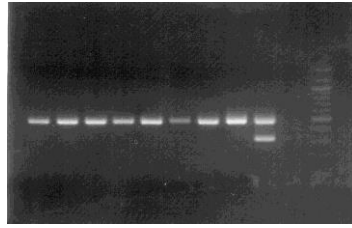


**Figure 8: Characteristic double bands for knockout mice as seen after electrophoresis.**

The sample in the ninth lane, but not the others, was from a heterozygous E2KO mice. The last lane contains the DNA ladder used to determine the size of the amplicons. The lane second to last contains an aliquot of the PCR reaction in which the genomic DNA template was replaced by water. That reaction was included in all experiments as a control for any contaminating PCR products from previous runs.

## **2.2 Isolation of adipose-derived stromal cells (ADSCs) from mice**

ADSCs were isolated according to previously described methods with slight modifications.<sup>104,109,110</sup> Briefly, the inguinal region of the examined mouse was firstly disinfected with isopropanol. Inguinal fat pads were then extracted with the aid of forceps and surgical knives. Fat pads were washed with 1x phosphate buffered saline (PBS) containing 100 units/mL penicillin and 100 units/mL streptomycin. Afterwards, fat pads were minced with sterilized blades and digested in a freshly prepared 25 mL solution of PBS with 0.075 % collagenase type 2 at 37°C for 30 minutes during rotation in a FisherBiotech Hybridization Incubator<sup>®</sup>. After digestion, the suspension was neutralized with 25 mL of high glucose Dulbecco's Modified Eagle Medium (DMEM), containing 10 % fetal bovine serum (FBS), 100 units/mL penicillin and 100 units/mL streptomycin. The suspension was then processed by a filtration through a 70- $\mu$ m mesh filter and a subsequent centrifugation [400x gravity (g), 10 minutes, 4°C]. After centrifugation, the floating fat was removed and precipitated cells were cultured.

### **2.3 Cell culture**

Isolated cells were cultured in a 24-well plate (500  $\mu$ L/well) with high glucose DMEM, supplemented with 10 % FBS, 100 units/mL penicillin and 100 units/mL streptomycin in humidified air with 5 % carbon dioxide (CO<sub>2</sub>) at 37°C. Initial cell seeding number averaged 100,000 cells per well. After 24 hours, non-adherent cells were once washed away with 500  $\mu$ L 1x PBS. The media was changed every three days and cells were subcultured before they got confluent. Cells were lifted off the culture dish by using 0.25 % trypsin-EDTA.

### **2.4 Adipogenic differentiation of ADSCs**

ADSCs were cultured until a sufficient cell number was available for differentiating subcultures. As soon as enough cells were cultured, they were lifted with 0.25 % trypsin-EDTA, counted with a hemocytometer and then subcultured into 48-well plates (in duplicates) with a seeding number of 35,000 to 50,000 ADSCs per well. Until confluence, cells were still cultured with high glucose DMEM, containing 10 % FBS, 100 units/mL penicillin and 100 units/mL streptomycin in humidified air with 5 % CO<sub>2</sub> at 37°C. Upon confluence, the basic media was removed and replaced by differentiation media.

According to protocols of our laboratory, adipogenic differentiation was induced by adipogenic media, which consisted of a 0.45  $\mu$ m-filtered alpha modification of Eagle's medium ( $\alpha$ MEM), containing 10 % FBS, 100 units/mL penicillin and 100 units/mL streptomycin and a final concentration of 5  $\mu$ g/mL insulin, 1  $\mu$ M rosiglitazone and 10<sup>-8</sup> M dexamethasone in humidified air with 5 % CO<sub>2</sub> at 37°C. Adipogenic media needed to be freshly prepared each time the media was replaced.

## 2.5 Total RNA extraction from ADSCs and RNA concentration measurement

Differentiation start was defined as “Day 0” of differentiation, when differentiation media containing insulin, rosiglitazone and dexamethasone was first applied to replace the basic media. Total RNA was harvested from “Day 0”, “Day 3”, “Day 6” and “Day 12” cell cultures treated with or without adipogenic differentiation factors in order to quantify adipogenic gene expression levels. RNeasy Plus Mini Kit<sup>®</sup> (QIAGEN) was used according to the supplied protocol for isolation and purification of total RNA. Finally, concentration of purified RNA was measured with the aid of a NanoDrop<sup>®</sup> spectrophotometer (Thermo Scientific) and diluted in sterile water to achieve the same RNA concentrations for all samples.

## 2.6 First-strand cDNA synthesis

Harvested RNA was reverse transcribed to first-strand cDNA using the kit SuperScript<sup>®</sup> III First-Strand Synthesis System (Invitrogen) according to the supplied protocol and yielded a 20- $\mu$ L reaction volume:

1  $\mu$ L of 50-250 ng random primers, 10 pg – 5  $\mu$ g total RNA (or 10 pg – 500 ng messenger ribonucleic acid [mRNA]) and 1  $\mu$ L 10 mM dNTP mixture were added into a nuclease-free microcentrifuge tube and filled up to 13  $\mu$ L with sterile, distilled water to be heated up to 65°C for five minutes. The mixture was thereafter cooled down on ice for at least one minute. 4  $\mu$ L 5x First-Strand Buffer, 1  $\mu$ L 0.1 M DTT, 1  $\mu$ L RNaseOUT<sup>™</sup> Recombinant RNase Inhibitor and 1  $\mu$ L SuperScript<sup>™</sup> III RT were added to the mixture and then followed by another cycle at 25°C for five minutes and a subsequent incubation at 50°C for 60 minutes. The mixture was then heated up to 70°C for 15 minutes to inactivate the reaction. Finally, RNase H was added and the mixture incubated at 37°C for 20 minutes to allow a removal of RNA complementary to the cDNA. Synthesized first-strand cDNA could then be processed as templates for a subsequent real-time quantitative reverse-transcription PCR.

## 2.7 Real-time quantitative reverse-transcription PCR (qRT-PCR)

To assess gene expression levels for certain investigated genes, we performed quantitative real-time reverse-transcription PCR (qRT-PCR), using QuantiTect SYBR Green RT-PCR Kits<sup>®</sup> (Qiagen) and StepOnePlus<sup>™</sup> Real-Time PCR System (Life Technologies - Applied Biosystems) as PCR instrument. qRT-PCR was performed according to the manufacturer's instructions.

For each investigated sample, a reaction mixture containing 20  $\mu$ L SYBR Green, 7  $\mu$ L ddH<sub>2</sub>O, 2  $\mu$ L uracil DNA glycosylase, 3  $\mu$ L cDNA sample and 8.25  $\mu$ L of the corresponding gene-specific primer mixture (each at 2.5  $\mu$ M) was prepared. Genes were amplified with the aid of various primers as specified in the table below (Table 5).

**Table 5: Primer sequences of different murine genes analysed by qRT-PCR.**

Gene name	Forward Primer	Reverse Primer
$\beta$ -actin	5' GATCTGGCACCACACCTTCT 3'	5' GGGGTGTTGAAGGTCTCAA 3'
Gsa	5' GCAGAAGGACAAGCAGGTCT 3'	5' CCCTCTCCGTAAACCCATT 3'
XLas	5' CTCATCGACAAGCAACTGGA 3'	5' CCCTCTCCGTAAACCCATT 3'
PPARg	5' GTGCCAGTTTCGATCCGTAGA 3'	5' GGCCAGCATCGTGTAGATGA 3'
aP2	5' ACACCGAGATTTCTTCAAAGTG 3'	5' CCATCTAGGGTTATGATGCTCTTCA 3'

$\beta$ -actin was used as reference gene and ddH<sub>2</sub>O instead of a template as negative control, allowing the detection of extraneous DNA.

## 2.8 Oil Red O staining

Prior to Oil Red O staining, cells were washed twice with PBS and fixed for 20 minutes at room temperature with 10 % formalin. Afterwards, cells were rinsed twice with ddH<sub>2</sub>O. A working solution of Oil Red O was diluted from a 0.5 % Oil Red O stock solution dissolved in isopropanol, i. e. three units of stock solution per two units of ddH<sub>2</sub>O (3:2), and filtered using a 0.22 micron syringe filter, applied to the cells and

incubated for 60 minutes at room temperature. Cells were washed three times with ddH<sub>2</sub>O and air dried for five minutes.

For evaluation, isopropanol was added and the cell culture plate put on a rotating plate for 10 minutes for Oil Red O elution. Standard curves were prepared and elutions collected to perform a spectrophotometric quantitation of Oil Red O staining by a microplate reader. Absorbance was read at 510 nm and data recorded with SoftMaxPro<sup>®</sup>.

## **2.9 Statistical analysis**

Data are expressed as mean  $\pm$  standard error of the mean (s.e.m). All experiments were performed at least in triplicate. The Student's t test (two-tailed) was performed by using raw data values, i. e. before any normalization, for comparing two means. In experiments quantifying the expression levels of adipogenic markers, there was marked variation in data among experiments. Therefore, we used a paired t-test to compare the values obtained from CD1 wt and E2KO ADSCs, i. e. values obtained from wild-type and E2KO genotype in a single experiment were paired. Observed differences between genotypes were considered statistically significant, if the p value was less than 0.05 ( $p < 0.05$ ). All statistical calculations were performed with the help of Microsoft Excel.



### 3 Results

#### 3.1 Gene expression measurements

##### 3.1.1 Expression levels of the alpha-subunit of the stimulatory G protein (G $\alpha$ ) in ADSCs from heterozygous E2KO mice vs. CD1 wt mice

On Day 0, i. e. prior to adipogenic differentiation, ADSCs both from CD1 wt and paternal E2KO mice were screened for G $\alpha$  expression levels. Five experiments per genotype were performed in order to determine G $\alpha$  expression, which was then averaged for each of the genotypes.  $\beta$ -actin was used as a reference gene and results of the qRT-PCR were expressed relative to the values of CD1 wt Day 0. Figure 9 shows that ADSCs from paternal E2KO mice have about half of the expression levels of G $\alpha$  compared to the levels in ADSCs from CD1 wt mice. This difference was statistically significant ( $p < 0.05$ ).

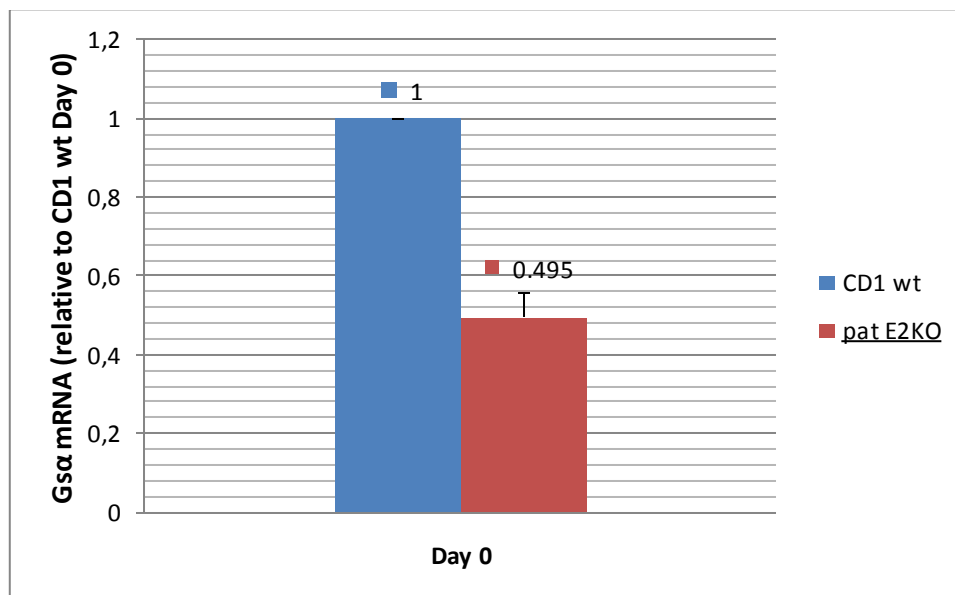


**Figure 9: G $\alpha$  mRNA expression in ADSCs from CD1 wt vs. pat E2KO mice. (n=5)**

Abbreviations: CD1 wt, CD1 wild-type; pat E2KO, paternal exon 2 knockout; G $\alpha$ , alpha-subunit of the stimulatory G protein; ADSCs, adipose-derived stromal cells.

Similarly, G $\alpha$  expression is reduced to about 47.4 % in ADSCs from maternal E2KO mice in comparison to ADSCs from CD1 wt mice, as shown in Figure 10. Again, this

difference was statistically significant ( $p < 0.05$ ). Four experiments were conducted to determine an averaged Gs $\alpha$  expression for each of the genotypes.

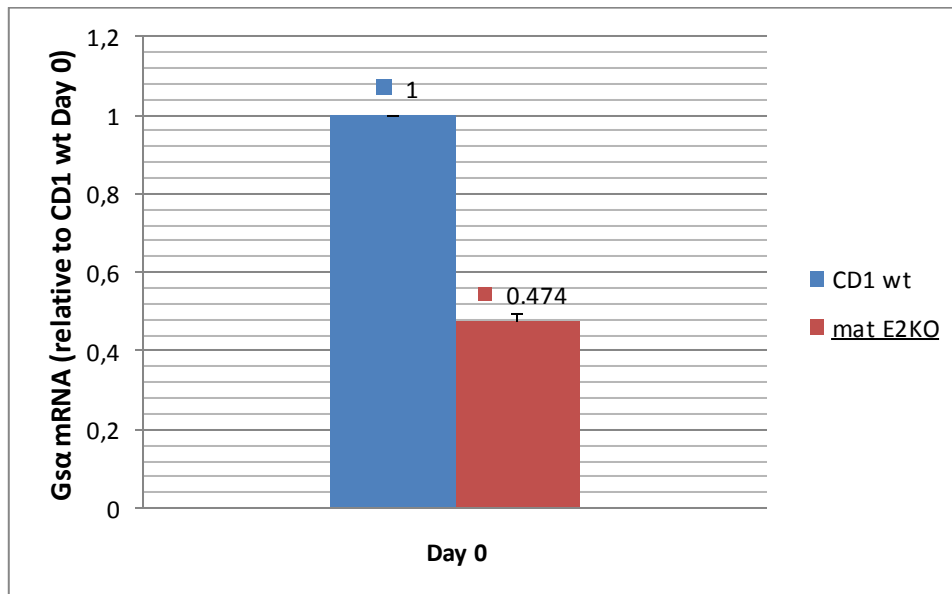


**Figure 10: Gs $\alpha$  mRNA expression in ADSCs from CD1 wt vs. mat E2KO mice. (n=4)**

Abbreviations: CD1 wt, CD1 wild-type; mat E2KO, maternal exon 2 knockout; Gs $\alpha$ , alpha-subunit of the stimulatory G protein; ADSCs, adipose-derived stromal cells.

### 3.1.2 Expression levels of the extra-large alpha-subunit (XL $\alpha$ s) in ADSCs from heterozygous E2KO mice vs. CD1 wt mice

Furthermore, we screened ADSCs from CD1 wt mice and from paternal E2KO mice for XL $\alpha$ s expression. Again, we conducted five experiments per genotype and averaged XL $\alpha$ s expression. Figure 11 displays markedly low expression of XL $\alpha$ s in ADSCs isolated from paternal E2KO mice as compared to ADSCs from CD1 wt mice, which show full expression of XL $\alpha$ s. This observed difference was statistically significant ( $p < 0.05$ ).

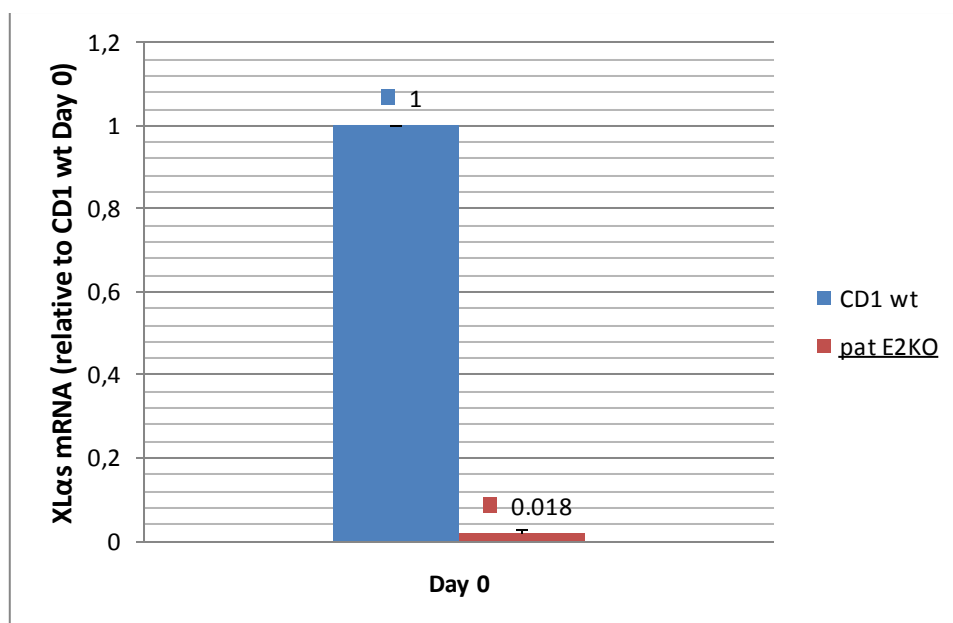


**Figure 11: XL $\alpha$ s mRNA expression in ADSCs from CD1 wt vs. pat E2KO mice. (n=5)**

Abbreviations: CD1 wt, CD1 wild-type; pat E2KO, paternal exon 2 knockout; XL $\alpha$ s, extra-large alpha-subunit (of the stimulatory G protein); ADSCs, adipose-derived stromal cells.

XL $\alpha$ s expression is elevated by about 40.1 % in ADSCs from maternal E2KO compared to same cells isolated from CD1 wt (Fig. 12) – even though equal expression is to be expected, but the observed difference was not statistically significant ( $p = 0.0511$ ). Four experiments were performed, expression levels for each genotype were averaged, and  $\beta$ -actin was used as a reference gene.

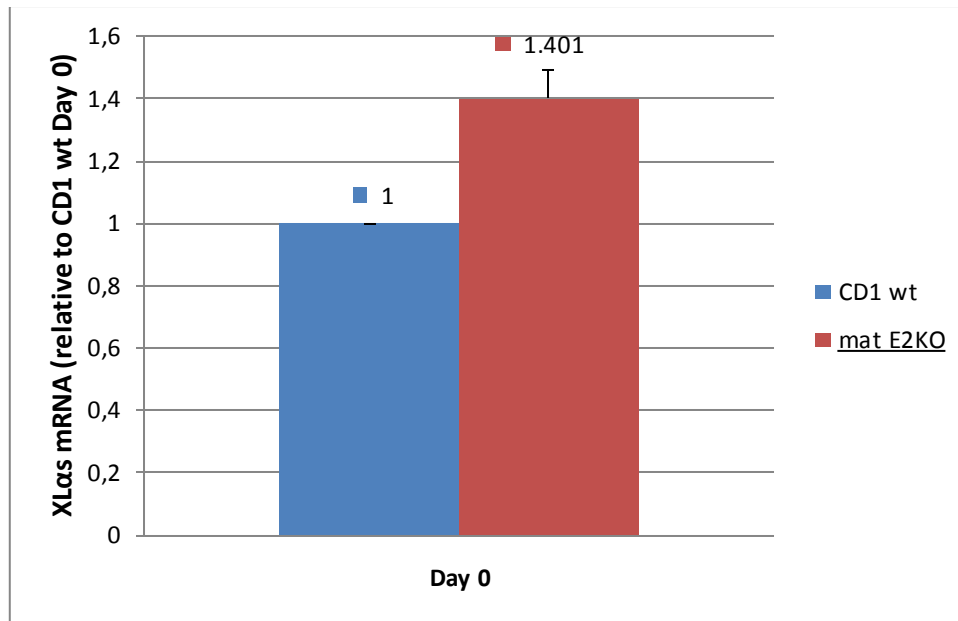


**Figure 12: XL $\alpha$ s mRNA expression in ADSCs from CD1 wt vs. mat E2KO mice. (n=4)**

Abbreviations: CD1 wt, CD1 wild-type; mat E2KO, maternal exon 2 knockout; XL $\alpha$ s, extra-large alpha-subunit (of the stimulatory G protein); ADSCs, adipose-derived stromal cells.

### 3.1.3 Expression levels of adipogenic markers in ADSCs from paternal E2KO mice vs. CD1 wt mice

#### 3.1.3.1 Expression of peroxisome proliferator-activated receptor gamma (PPAR $\gamma$ )

Peroxisome proliferator-activated receptor gamma (PPAR $\gamma$ ) was used as one of two adipogenic markers in order to assess adipogenic differentiation. As a second adipogenic marker, we used lipid-binding protein (aP2). PPAR $\gamma$  is expressed primarily in early adipogenic differentiation. It is therefore used as a very early differentiation marker, while aP2 is a late differentiation marker.

We isolated ADSCs in four single experiments (n=4). These ADSCs were cultured to proliferate and subsequently differentiated (in duplicates per value) for a total number of 12 days, with Day 0 being the starting point for the adipogenic differentiation, thus representing the base level expression without differentiation. We determined PPAR $\gamma$

mRNA expression levels in ADSCs from CD1 wt and paternal E2KO mice in each experiment and averaged the data obtained from multiple experiments.

In Figure 13, absolute PPAR $\gamma$  mRNA expression in ADSCs derived from CD1 wt and paternal E2KO mice is shown. Results of the qRT-PCR were expressed relative to  $\beta$ -actin that was used as a reference gene. On Day 0, prior to differentiation, absolute PPAR $\gamma$  mRNA levels are about 3.8-fold higher in ADSCs from the knockout compared to CD1 wt Day 0, but the observed difference was not statistically significant ( $p = 0.1393$ ). The expression levels in the CD1 wt mice (blue line) rise until Day 6 of differentiation, with absolute PPAR $\gamma$  mRNA expression being about 0.0012, i. e. more than nine times higher as compared to CD1 wt Day 0 levels under adipogenic conditions. Day 6 is likewise a turning point as absolute PPAR $\gamma$  mRNA expression levels on Day 12 are declined to about 0.0004, i. e. less than threefold the levels compared to Day 0.

In contrast, absolute PPAR $\gamma$  mRNA expression levels in ADSCs derived from paternal E2KO (green line) increase to about 0.0014, i. e. about 2.8-fold levels on Day 3 as compared to paternal E2KO Day 0 levels, and thereafter decrease to about 0.0009 on Day 12, i. e. less than two-fold levels as compared to paternal E2KO Day 0 levels.

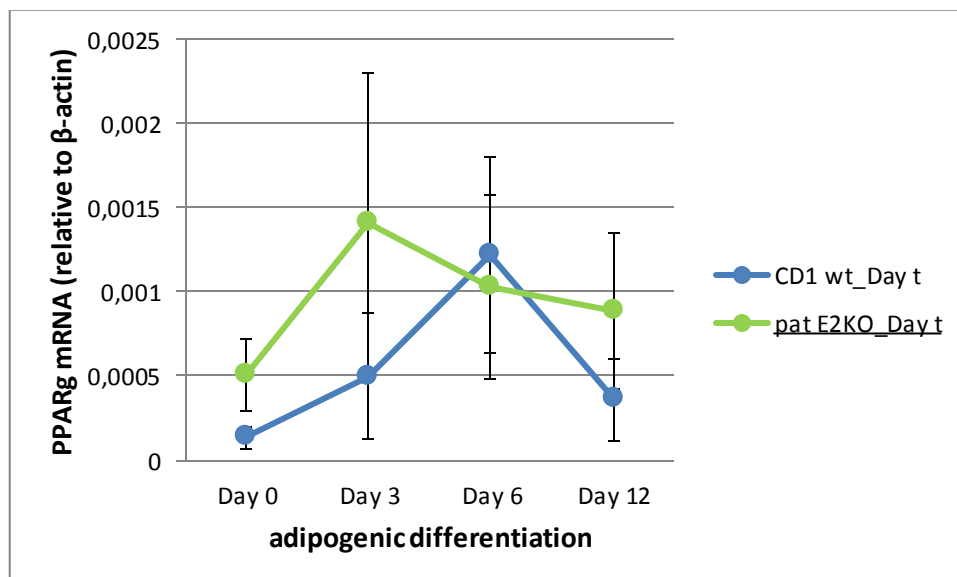


**Figure 13: Absolute PPAR $\gamma$  mRNA expression in ADSCs from CD1 wt vs. pat E2KO mice. (n=4)**

Abbreviations: CD1 wt, CD1 wild-type; pat E2KO, paternal exon 2 knockout; PPAR $\gamma$ , peroxisome proliferator-activated receptor gamma; ADSCs, adipose-derived stromal cells.

Looking at the standard error of the mean (s.e.m.), Day 6 exhibits the highest variation for CD1 wt and Day 3 the highest variation for paternal E2KO throughout the differentiation period with an error (=percentage of the s.e.m. relative to the mean value) of approximately 47.6 % for CD1 wt and about 63.8 % for paternal E2KO, respectively.

Figure 14 demonstrates the same data set of PPAR $\gamma$  mRNA expression levels in ADSCs derived from CD1 wt and paternal E2KO mice, but being normalized to Day 0 levels of CD1 wt, as was done in the published study by Liu et al.<sup>65</sup> On Day 0, prior to differentiation, normalized PPAR $\gamma$  mRNA levels are elevated in ADSCs from the knockout by about 3.8-fold compared to CD1 wt Day 0. PPAR $\gamma$  mRNA expression levels for CD1 wt increase on Day 3 and grow especially on Day 6, finally decreasing then on Day 12. Normalized values are about 3.7 on Day 3, about 9.2 on Day 6 and about 2.7 on Day 12.

PPAR $\gamma$  mRNA expression levels of paternal E2KO ADSCs normalized to Day 0 of CD1 wt show about 3.8-fold PPAR $\gamma$  mRNA expression levels as compared to Day 0 of CD1 wt, i. e. prior to differentiation. Until Day 3, PPAR $\gamma$  mRNA expression levels of paternal E2KO ADSCs normalized to Day 0 of CD1 wt exhibit an increase with about 10.6-fold levels and thereafter gradually decrease to about 7.8-fold levels on Day 6 and about 6.7-fold levels on Day 12. Throughout the differentiation period except for Day 6, PPAR $\gamma$  mRNA expression levels of paternal E2KO ADSCs normalized to Day 0 of CD1 wt are above the CD1 wt growth rate for PPAR $\gamma$  mRNA expression levels.

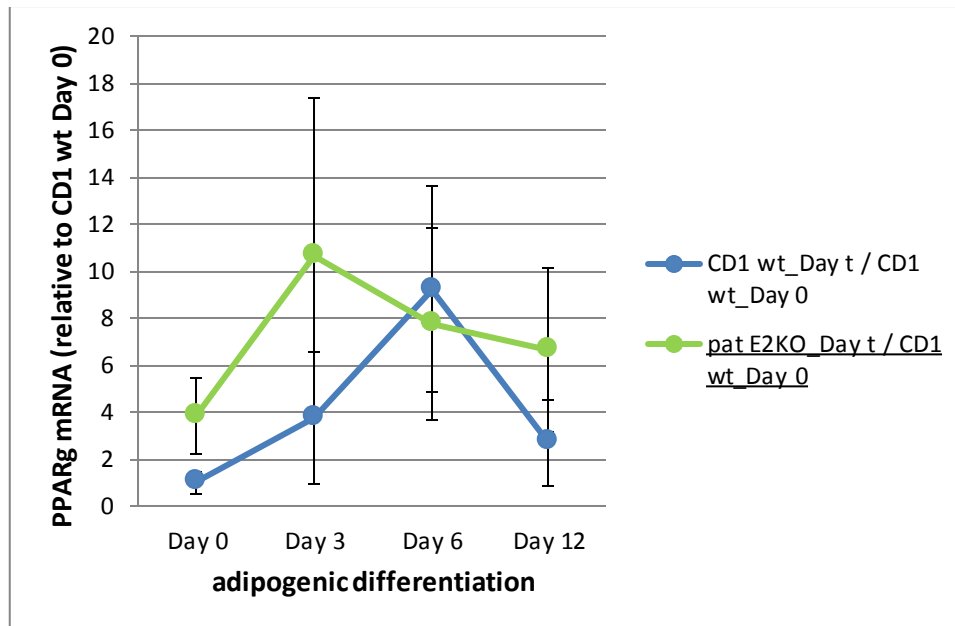


**Figure 14: PPAR $\gamma$  mRNA expression in ADSCs from CD1 wt vs. pat E2KO mice each normalized to CD1 wt Day 0. (n=4)** Abbreviations: CD1 wt, CD1 wild-type; pat E2KO, paternal exon 2 knockout; PPAR $\gamma$ , peroxisome proliferator-activated receptor gamma; ADSCs, adipose-derived stromal cells.

Again, highest s.e.m. value regarding CD1 wt can be detected on Day 6 of differentiation with an error of about 47.6 %. Looking at the paternal E2KO values normalized to wild-type Day 0, s.e.m. values are quite high, the highest being on Day 3 with an error level around 63.8 %.

### 3.1.3.2 Expression of lipid-binding protein (aP2)

Lipid-binding protein (aP2) was used as a second marker for adipogenic differentiation. We used the same RNA from the previous four experiments for determination of aP2 mRNA expression levels in ADSCs from CD1 wt and paternal E2KO mice. The data obtained from multiple experiments was averaged once again, being presented in absolute (Fig. 15) or normalized values (Fig. 16).

Figure 15 shows the absolute mRNA expression levels of aP2 in ADSCs from CD1 wt and paternal E2KO mice. Results of the qRT-PCR were expressed relative to  $\beta$ -actin that was used as a reference gene. Throughout the whole differentiation period, absolute aP2 mRNA expression levels are generally higher in the knockout mice

compared to their wild-type littermates. Peaks of absolute aP2 mRNA expression in the knockout mice have been observed for Day 3, Day 6 and Day 12 of adipogenic differentiation with levels up to around 0.3986, 0.4093 and 0.3652, respectively, i. e. more than 11 times of the paternal E2KO levels of Day 0.

Absolute mRNA expression levels of aP2 in ADSCs from CD1 wt rise from about 0.2627 on Day 3 to about 0.3488 on Day 12, i. e. about 25.4-fold levels on Day 3 to about 33.7-fold levels on Day 12 of differentiation as compared to CD1 Day 0 levels.

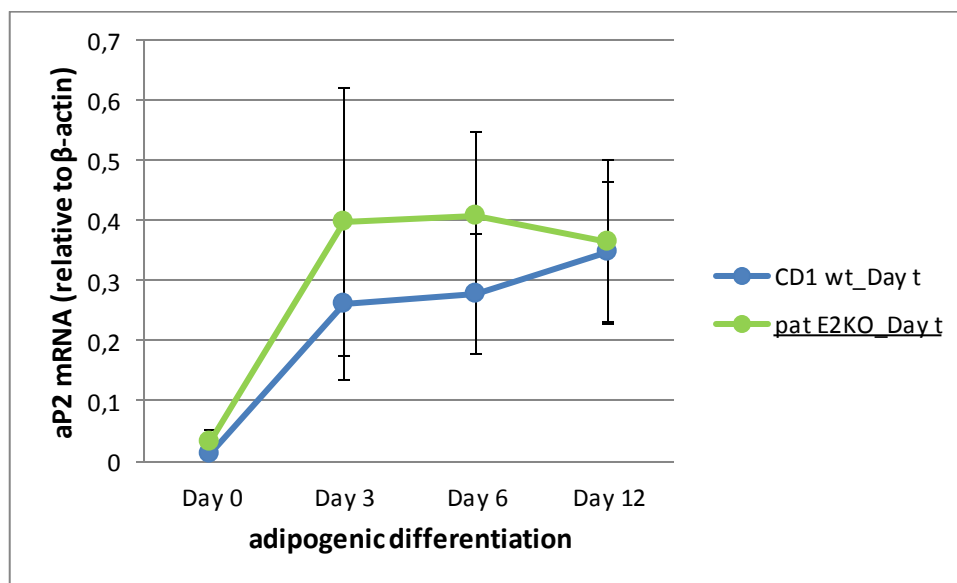


**Figure 15: Absolute aP2 mRNA expression in ADSCs from CD1 wt vs. pat E2KO mice. (n=4)**

Abbreviations: CD1 wt, CD1 wild-type; pat E2KO, paternal exon 2 knockout; aP2, adipocyte lipid-binding protein 2; ADSCs, adipose-derived stromal cells.

Variation can be detected on all of the examined differentiation days. Maximum s.e.m. values occur on Day 3 for both genotypes with errors of about 48.7 % for the wild-type and 55.9 % for the knockout, respectively. The observed difference on Day 3 was not statistically significant ( $p = 0.6159$ ).

In Figure 16, the changes in aP2 mRNA expression levels from CD1 wt mice are compared to aP2 mRNA expression levels in ADSCs from paternal E2KO normalized to the Day 0 aP2 expression levels of ADSCs from CD1 wt mice. On Day 0, prior to differentiation, normalized PPAR $\gamma$  mRNA levels are elevated in ADSCs from the knockout with about 3.2-fold compared to CD1 wt Day 0. Throughout the whole differentiation period, aP2 mRNA expression levels in ADSCs from paternal E2KO mice



normalized to Day 0 of CD1 wt tended to be generally higher compared to the CD1 growth rate. ADSCs from paternal E2KO mice normalized to wild-type Day 0 levels show an increase in aP2 mRNA expression levels on Day 3 with about 38.6-fold high levels that remain on a similar level on Day 6 and Day 12, i. e. 39.6-fold high levels and 35.3-fold high levels, respectively.

aP2 mRNA expression levels in ADSCs from CD1 wt mice rise up to about 25.4-fold levels on Day 3 and show maximum aP2 expression levels on Day 12 of differentiation with about 33.7-fold levels.

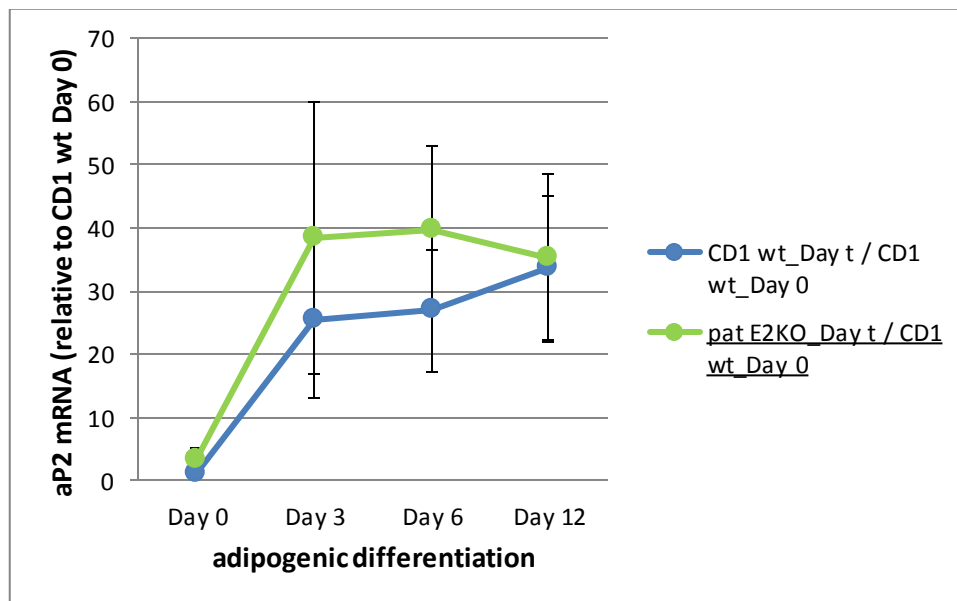


**Figure 16: aP2 mRNA expression in ADSCs from CD1 wt vs. pat E2KO mice each normalized to CD1 wt Day 0. (n=4)** Abbreviations: CD1 wt, CD1 wild-type; pat E2KO, paternal exon 2 knockout; aP2, adipocyte lipid-binding protein 2; ADSCs, adipose-derived stromal cells.

Again, maximum s.e.m. values occur on Day 3 for both genotypes with errors of about 48.7 % for the wild-type and 55.9 % for the knockout, respectively.

### 3.1.4 Expression levels of adipogenic markers in ADSCs from maternal E2KO mice vs. CD1 wt mice

#### 3.1.4.1 Expression of peroxisome proliferator-activated receptor gamma (PPAR $\gamma$ )

Methodically identical RNA assays were performed with ADSCs from CD1 wt and maternal E2KO mice. Peroxisome proliferator-activated receptor gamma (PPAR $\gamma$ ) was used once again as one of two adipogenic markers.

Results of the qRT-PCR were expressed relative to  $\beta$ -actin. ADSCs from CD1 wt and paternal E2KO mice exhibit a similar trend with regard to their absolute mRNA expression levels (Fig. 17). Peaks of absolute PPAR $\gamma$  mRNA expression can be observed on Day 3 with about 0.0082 for wild-type and about 0.0100 for maternal E2KO, i. e. about 99.7-fold and about 188.3-fold increase over genotype-specific Day 0 absolute PPAR $\gamma$  mRNA expression levels. Day 6 and Day 12 show a gradual decrease in absolute PPAR $\gamma$  mRNA expression levels with about 0.0015 for CD1 wt and about 0.0010 for maternal E2KO, i. e. about 17.9-fold and about 18.7-fold increase as compared to genotype-specific Day 0 levels, respectively.

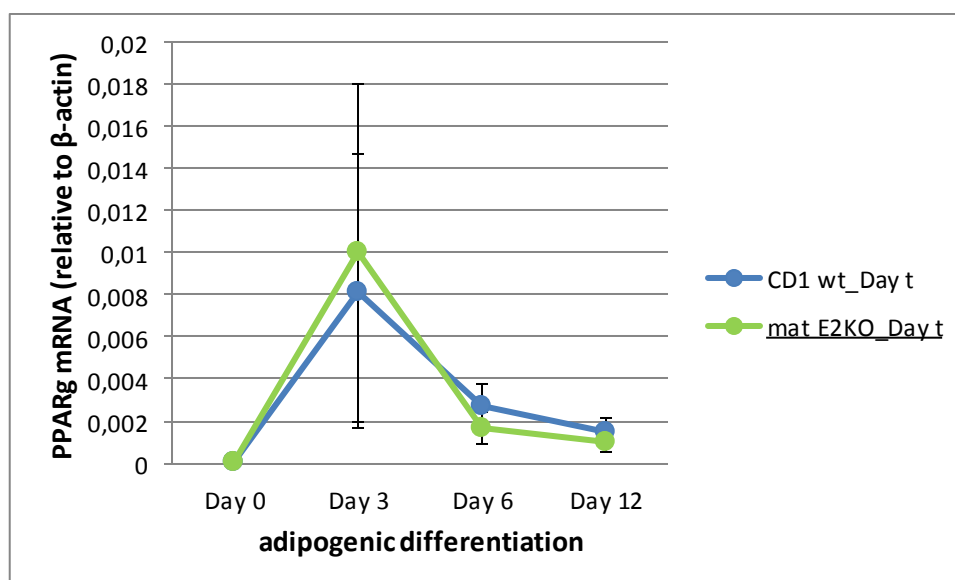


**Figure 17: Absolute PPAR $\gamma$  mRNA expression in ADSCs from CD1 wt vs. mat E2KO mice. (n=4, except for Day 3 with n=3)** Abbreviations: CD1 wt, CD1 wild-type; mat E2KO, maternal exon 2 knockout; PPAR $\gamma$ , peroxisome proliferator-activated receptor gamma; ADSCs, adipose-derived stromal cells.

Maximum s.e.m. values for both genotypes are obtained on Day 3, with errors of about 79.9 % for CD1 wt and 80.5 % for maternal E2KO, respectively.

A comparison of PPAR $\gamma$  mRNA expression levels normalized to CD1 wt Day 0 for each genotype indicates that both CD1 wt and maternal E2KO ADSCs have again highest PPAR $\gamma$  mRNA expression levels on Day 3 (Fig. 18). PPAR $\gamma$  mRNA expression levels in the wild-type background rise to approximately 99.7-fold of the starting value, while the corresponding PPAR $\gamma$  mRNA expression levels of ADSCs from maternal E2KO mice rise to about 122-fold of the starting value. Towards Day 12, genotype-specific PPAR $\gamma$  mRNA expression levels tended to decrease with about 17.9-fold for ADSCs from CD1 wt mice and about 12.1-fold in the knockout background.

In general, Fig. 17 and Fig. 18 show a stable genotype-independent trend and similar PPAR $\gamma$  mRNA expression levels with only minor differences in ADSCs from CD1 wt and maternal E2KO mice as compared to the more random course of the PPAR $\gamma$  mRNA expression curve in the paternal E2KO experiments (Fig. 13 and Fig. 14). In addition, absolute PPAR $\gamma$  mRNA expression in the maternal E2KO experiments (Fig. 17) as compared to the paternal E2KO experiments (Fig. 13) is in relation much higher.

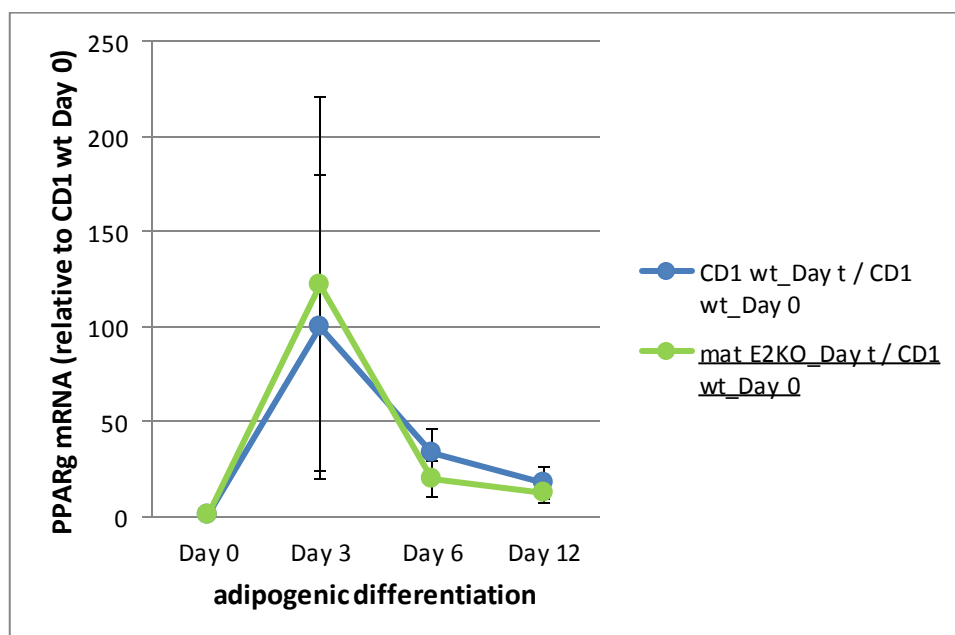


**Figure 18: PPAR $\gamma$  mRNA expression in ADSCs from CD1 wt vs. mat E2KO mice each normalized to CD1 wt Day 0. (n=4, except for Day 3 with n=3)** Abbreviations: CD1 wt, CD1 wild-type; mat E2KO, maternal exon 2 knockout; PPAR $\gamma$ , peroxisome proliferator-activated receptor gamma; ADSCs, adipose-derived stromal cells.

With regard to the expression profile in CD1 wt, errors are about 79.9 % on Day 3, about 38.6 % on Day 6 and about 46.9 % on Day 12 of differentiation. On the other hand, maternal E2KO data normalized to CD1 wt levels of Day 0 show errors of approximately 80.5 % on Day 3, about 46.7 % on Day 6 and about 46.7 % on Day 12 of differentiation. Again the variation in the data was quite high, and the differences observed on Day 3 were not statistically significant ( $p = 0.87$ ).

### **3.1.4.2 Expression of lipid-binding protein (aP2)**

Lipid-binding protein (aP2) was again used as a second marker for adipogenic differentiation.

Figure 19 displays absolute aP2 mRNA expression levels in ADSCs from maternal E2KO mice as opposed to CD1 wt mice. Results of the qRT-PCR were expressed relative to  $\beta$ -actin. Throughout the whole differentiation period absolute aP2 mRNA expression levels are lower in ADSCs from maternal E2KO mice as compared to absolute aP2 mRNA expression levels of wild-type background. Both genotypes exhibit a similar trend with peaks of absolute aP2 mRNA expression levels on Day 3. ADSCs from CD1 wt mice show absolute aP2 mRNA expression levels around 2.4869 on Day 3, about 1.0401 on Day 6 and about 0.8172 on Day 12, i. e. 347.3-fold levels on Day 3, 145.2-fold levels on Day 6 and 114.1-fold levels on Day 12 as compared to Day 0. On the other hand, ADSCs from maternal E2KO mice feature absolute aP2 mRNA expression levels that are about 1.9587 on Day 3, about 0.6947 on Day 6 and about 0.5673 on Day 12, i. e. about 550.9-fold high levels on Day 3, about 195.4-fold high levels on Day 6 and about 159.6-fold high levels on Day 12 of differentiation as compared to maternal E2KO Day 0 levels.

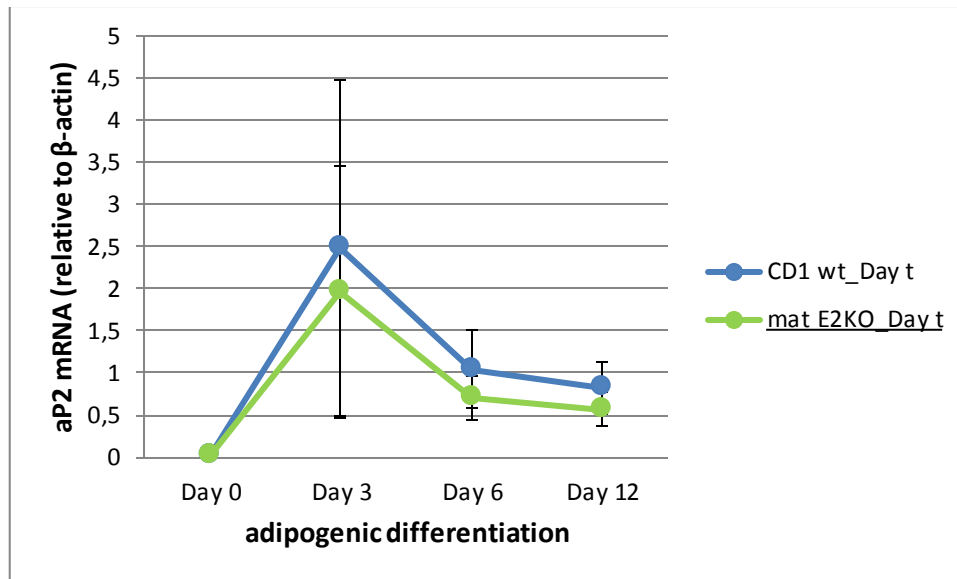


**Figure 19: Absolute aP2 mRNA expression in ADSCs from CD1 wt vs. mat E2KO mice. (n=4, except for Day 3 with n=3)** Abbreviations: CD1 wt, CD1 wild-type; mat E2KO, maternal exon 2 knockout; aP2, adipocyte lipid-binding protein 2; ADSCs, adipose-derived stromal cells.

Again, highest s.e.m. values for both genotypes can be detected on Day 3 of differentiation with errors of about 80.7 % for CD1 wt and 76.6 % for maternal E2KO, respectively.

Figure 20 depicts the normalization of day-specific aP2 mRNA expression levels in ADSCs from CD1 wt and maternal E2KO mice to Day 0 levels of CD1 wt. Again, peaks of aP2 mRNA expression levels can be observed for both genotypes on Day 3 of differentiation. Normalized aP2 mRNA expression levels in the wild-type rise to about 347.3-fold levels on Day 3, while normalized aP2 mRNA expression levels in the knockout rise to approximately 273.5-fold levels on Day 3. Towards Day 12, the aP2 mRNA expression levels in CD1 wt ADSCs decrease to about 114.1-fold, and those in maternal E2KO to about 79.2-fold.

Again, Fig. 19 and Fig. 20 show a stable genotype-independent trend and similar aP2 mRNA expression levels with only minor differences in ADSCs from CD1 wt and maternal E2KO mice as compared to the more random course of the aP2 mRNA expression curve in the paternal E2KO experiments (Fig. 15 and Fig. 16). Furthermore, absolute aP2 mRNA expression in the maternal E2KO experiments (Fig. 19) is again much higher as compared to the paternal E2KO experiments (Fig. 15).

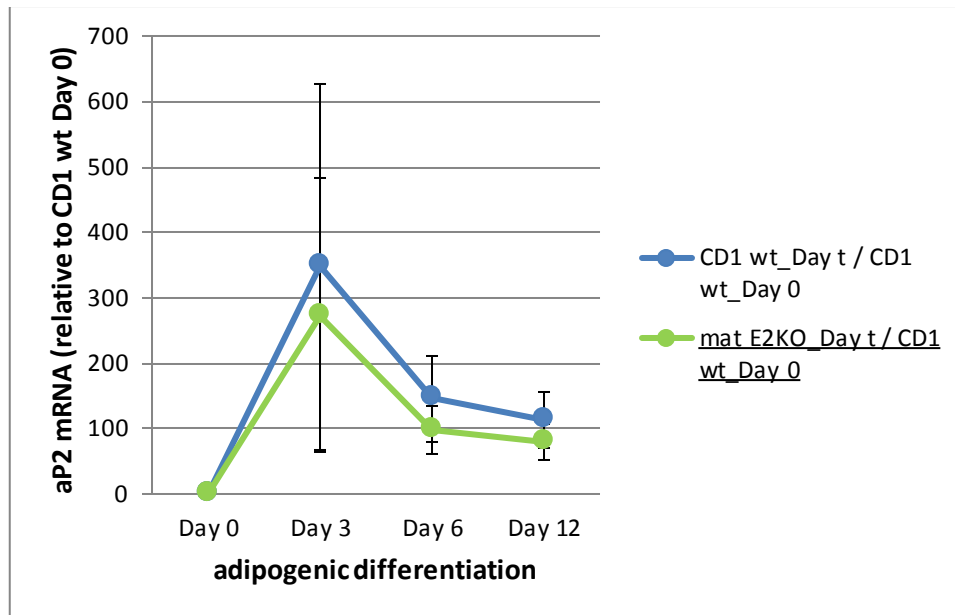


**Figure 20: aP2 mRNA expression in ADSCs from CD1 wt vs. mat E2KO mice each normalized to CD1 wt Day 0. (n=4, except for Day 3 with n=3)** Abbreviations: CD1 wt, CD1 wild-type; mat E2KO, maternal exon 2 knockout; aP2, adipocyte lipid-binding protein 2; ADSCs, adipose-derived stromal cells.

Variation for the CD1 wt-specific trend in aP2 mRNA expression shows errors of about 80.7 %, 44.6 % and 37.3 % for Days 3, 6 and 12, respectively. On the other hand, maternal E2KO data normalized to CD1 wt Day 0 levels show errors of about 76.6 % for Day 3, about 38.0 % on Day 6 and about 35.9 % on Day 12 of differentiation. Because of the high s.e.m. values, it is hard to determine whether the differences are real or have occurred by chance.

### 3.1.5 Comparison of expression levels of adipogenic markers in ADSCs from CD1 wt mice between experiments

#### 3.1.5.1 Expression of peroxisome proliferator-activated receptor gamma (PPAR $\gamma$ )

In Figure 21, we compared absolute PPAR $\gamma$  mRNA expression levels in ADSCs from CD1 wt mice between the two main experimental set-ups, i. e. paternal E2KO vs. CD1 wt and maternal E2KO vs. CD1 wt. The following figure displays absolute PPAR $\gamma$  mRNA expression levels in ADSCs from CD1 wt mice used in the maternal vs. paternal

E2KO experiments. The results show that wild-type ADSCs in maternal E2KO experiments have about 16.5-fold, about 2.2-fold and about 4.1-fold higher PPAR $\gamma$  mRNA expression levels on Days 3, 6, and 12, respectively, than the wild-type ADSCs used in paternal E2KO experiments, although the differences were not statistically significant. Note that equal PPAR $\gamma$  mRNA expression levels and similar differentiation trends are expected in wild-type ADSCs in both paternal and maternal E2KO experiments.

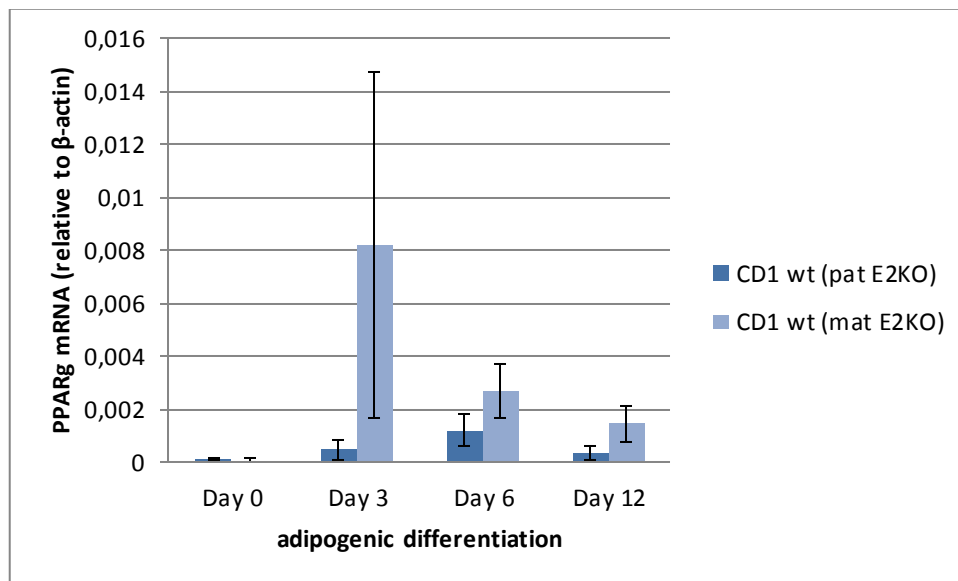


**Figure 21: Absolute PPAR $\gamma$  mRNA expression in ADSCs from CD1 wt mice. (n=4, except for Day 3 of CD1 wt\_Day t (mat E2KO) with n=3)** Abbreviations: CD1 wt, CD1 wild-type; pat E2KO, paternal exon 2 knockout; mat E2KO, maternal exon 2 knockout; PPAR $\gamma$ , peroxisome proliferator-activated receptor gamma; ADSCs, adipose-derived stromal cells.

Errors in the absolute PPAR $\gamma$  mRNA expression levels in ADSCs from CD1 wt used in the paternal E2KO experiments are about 75.7 % on Day 3, about 47.6% on Day 6 and about 68 % on Day 12, while those used in the maternal E2KO experiments are about 79.9 %, about 38.6 % and about 46.9 %, respectively.

### 3.1.5.2 Expression of lipid-binding protein (aP2)

Figure 22 shows that absolute aP2 mRNA expression levels in ADSCs from CD1 wt mice used in the maternal E2KO experiments are about 9.5-fold, about 3.7-fold and about 2.3-fold higher on Days 3, 6, and 12, respectively, as compared to the corresponding absolute aP2 mRNA expression levels in ADSCs from CD1 wt mice used in the paternal E2KO experiments, although the differences were not statistically significant. Again, equal aP2 mRNA expression levels and similar trends are expected in wild-type ADSCs in both paternal and maternal E2KO experiments.

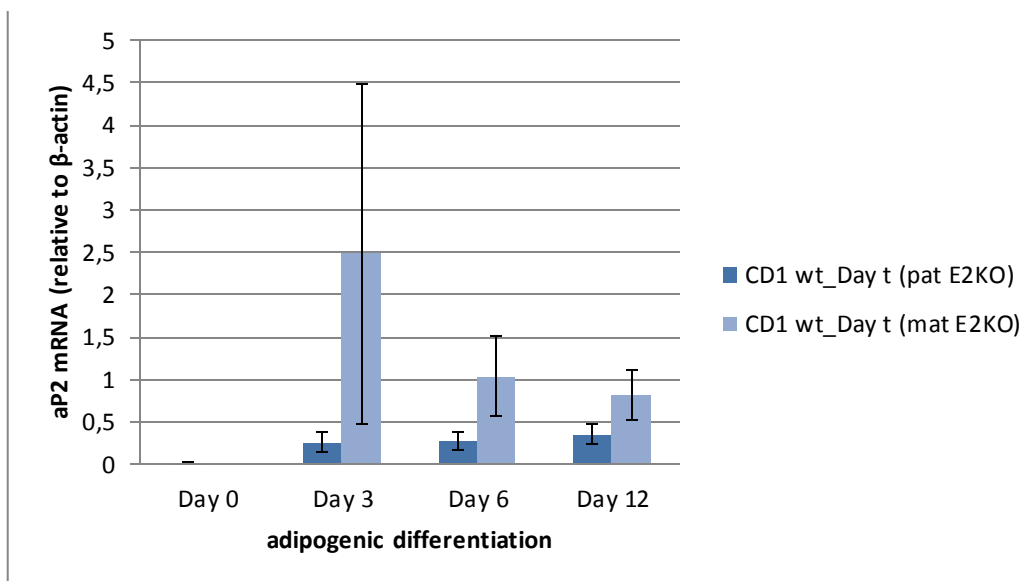


**Figure 22: Absolute aP2 mRNA expression in ADSCs from CD1 wt mice. (n=4, except for Day 3 of CD1 wt\_Day t (mat E2KO) with n=3)** Abbreviations: CD1 wt, CD1 wild-type; pat E2KO, paternal exon 2 knockout; mat E2KO, maternal exon 2 knockout; aP2, adipocyte lipid-binding protein 2; ADSCs, adipose-derived stromal cells.

Errors in the absolute aP2 mRNA expression levels in ADSCs from CD1 wt used in the paternal E2KO experiments are about 48.7 % on Day 3, about 35.8 % on Day 6 and about 33.6 % on Day 12, while those used in the maternal E2KO experiments are about 80.1 %, about 44.6 % and about 37.3 %, respectively.



### 3.2 Oil Red O results

In order to re-confirm trends by an alternative experiment, we further conducted staining experiments with Oil Red O. After isolation and cultivation of ADSCs, the Oil Red O staining was performed on Day 7 of adipogenic differentiation.

#### 3.2.1 Oil Red O elution in ADSCs from paternal E2KO mice vs. CD1 wt mice

Comparing amounts of eluted Oil Red O from CD1 wt and paternal E2KO ADSCs, one can detect an about 2.22-fold elevated amount of Oil Red O in ADSCs from paternal E2KO mice on Day 7 (Fig. 23). The value for the knockout normalized to wild-type tended to be higher than in the wild-type, but the observed difference was not statistically significant ( $p = 0.10$ ). Staining experiments were performed three times per genotype and spectrophotometric quantitation of Oil Red O staining was expressed relative to the values of CD1 wt Day 7. The error in the paternal E2KO normalized to the CD1 wt value is about 28.8 %.

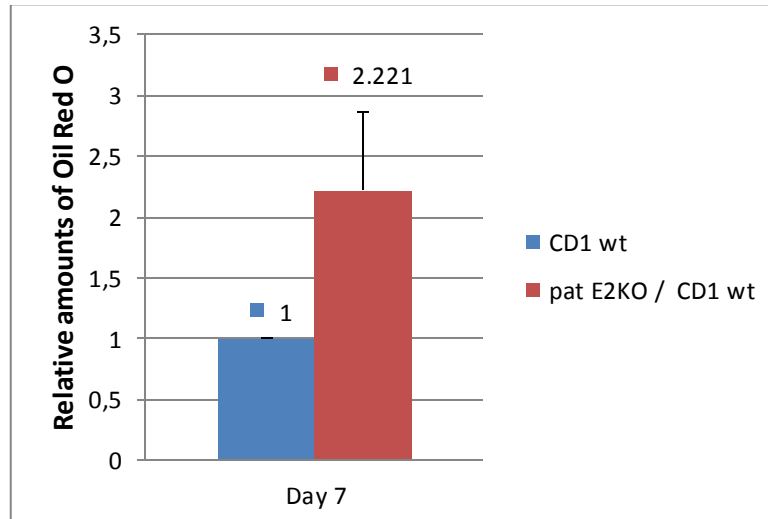


**Figure 23: Relative amounts of Oil Red O in ADSCs from CD1 wt vs. pat E2KO mice normalized to CD1 wt. (n=3)** Abbreviations: CD1 wt, CD1 wild-type; pat E2KO, paternal exon 2 knockout; ADSCs, adipose-derived stromal cells.

The following figures show pictures of stained wells within the scope of our Oil Red O experiments, both for CD1 wt as well as paternal E2KO. In all of the three experiments (Fig. 24, Fig. 25 and Fig. 26) an increased staining of lipid vacuoles can be observed in ADSCs isolated from paternal E2KO (Fig. 24, A2/B2; Fig. 25, A4/B4; Fig. 26, A6/B6) as opposed to CD1 wt mice (Fig. 24, A1/B1; Fig. 25, A3/B3; Fig. 26, A5/B5).

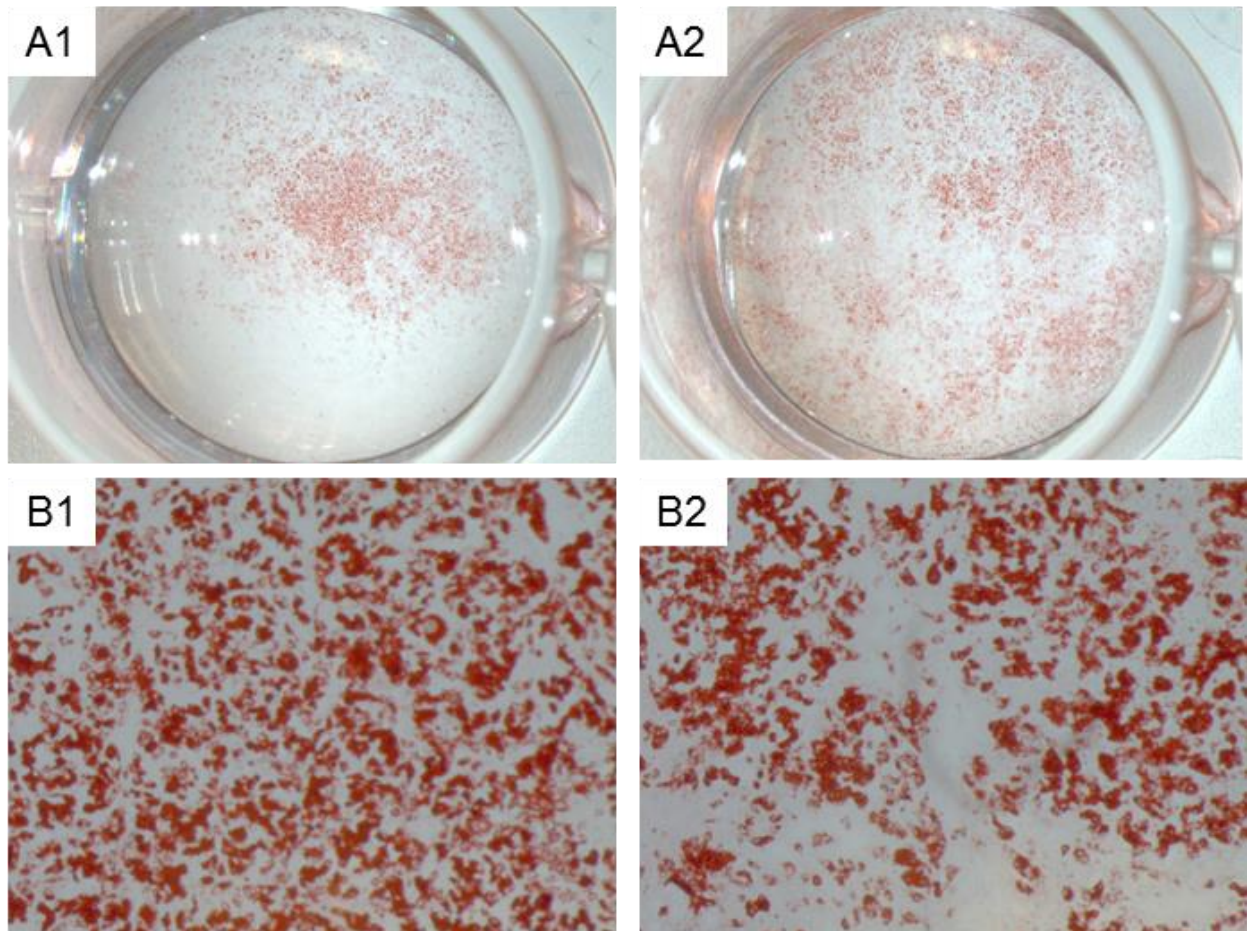


**Figure 24: Oil Red O staining of CD1 wt and pat E2KO ADSCs on Day 7 of adipogenic differentiation. (experiment #38)**

(A1) CD1 wt, 1x amplification. (A2) Pat E2KO, 1x amplification.

(B1) CD1 wt, 10x amplification. (B2) Pat E2KO, 10x amplification.

Abbreviations: CD1 wt, CD1 wild-type; pat E2KO, paternal exon 2 knockout; ADSCs, adipose-derived stromal cells.

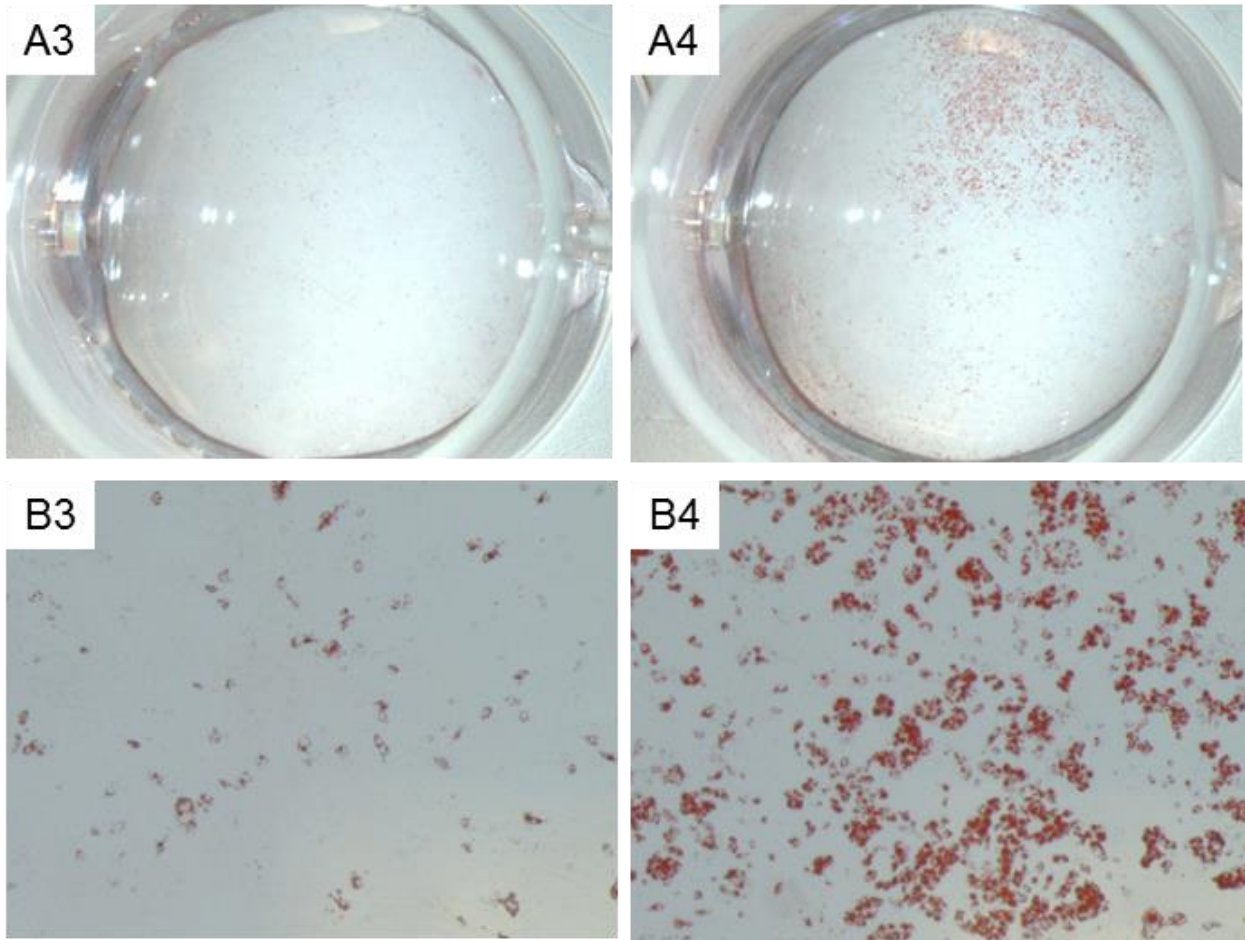


**Figure 25: Oil Red O staining of CD1 wt and pat E2KO ADSCs on Day 7 of adipogenic differentiation. (experiment #43)**

(A3) CD1 wt, 1x amplification. (A4) Pat E2KO, 1x amplification.

(B3) CD1 wt, 10x amplification. (B4) Pat E2KO, 10x amplification.

Abbreviations: CD1 wt, CD1 wild-type; pat E2KO, paternal exon 2 knockout; ADSCs, adipose-derived stromal cells.

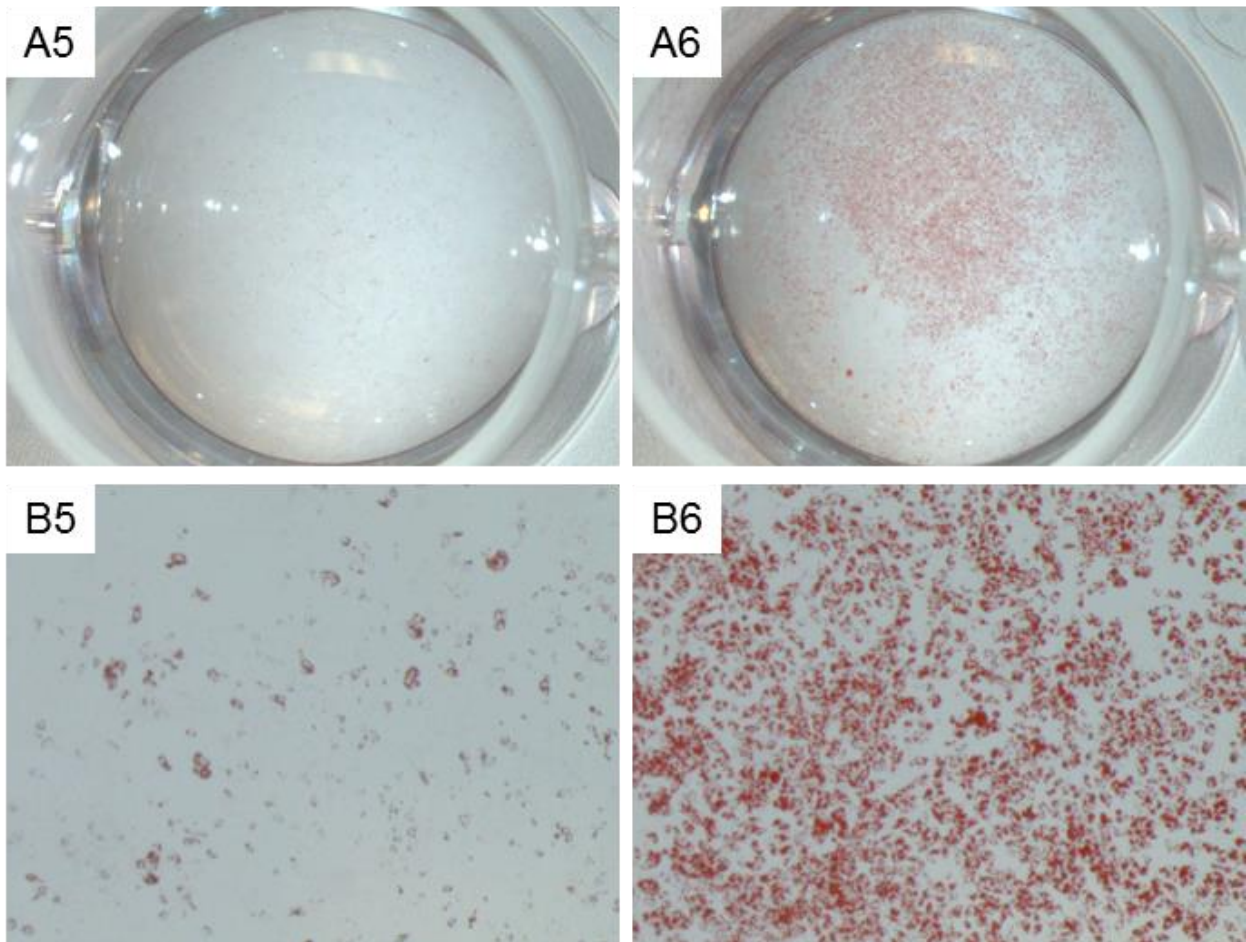


**Figure 26: Oil Red O staining of CD1 wt and pat E2KO ADSCs on Day 7 of adipogenic differentiation. (experiment #46)**

(A5) CD1 wt, 1x amplification. (A6) Pat E2KO, 1x amplification.

(B5) CD1 wt, 10x amplification. (B6) Pat E2KO, 10x amplification.

Abbreviations: CD1 wt, CD1 wild-type; pat E2KO, paternal exon 2 knockout; ADSCs, adipose-derived stromal cells.

### **3.2.2 Oil Red O elution in ADSCs from maternal E2KO mice vs. CD1 wt mice**

Staining of ADSCs from CD1 wt and maternal E2KO with Oil Red O and a subsequent quantitation of the Oil Red O elution on Day 7 exhibits an approximately 1.24-fold higher amount of Oil Red O in maternal E2KO cells as compared to cells isolated from wild-type littermates (Fig. 27). The observed difference was not statistically significant ( $p = 0.90$ ). Staining experiments have been performed three times per genotype and spectrophotometric quantitation of Oil Red O staining was expressed relative to the values of CD1 wt Day 7.

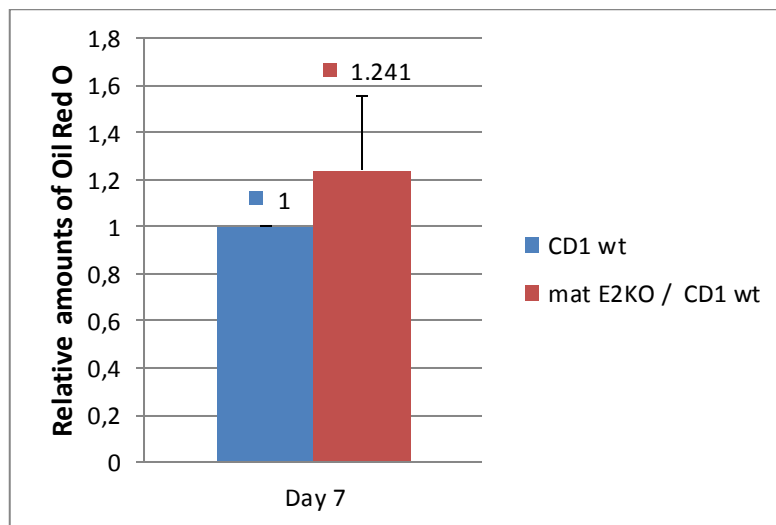


**Figure 27: Relative amounts of Oil Red O in ADSCs from CD1 wt vs. mat E2KO mice normalized to CD1 wt. (n=3)** Abbreviations: CD1 wt, CD1 wild-type; mat E2KO, maternal exon 2 knockout; ADSCs, adipose-derived stromal cells.

The error in the maternal E2KO normalized to the CD1 wt value is about 25.1 %.

Oil Red O stainings for ADSCs isolated from maternal E2KO mice and their wild-type littermates are shown in the following figures. In Figure 29, one can observe more Oil Red O staining of lipid vacuoles for the knockout, i. e. for ADSCs isolated from maternal E2KO mice (Fig. 29, A4/B4) compared to CD1 wt littermates (Fig. 29, A3/B3). Note, however, that an increase in Oil Red O staining was not observed in all the experiments (Fig. 28 and Fig. 30), and this is reflected in the finding that the difference between wild-type and maternal E2KO littermates is not significant (see Fig. 27).

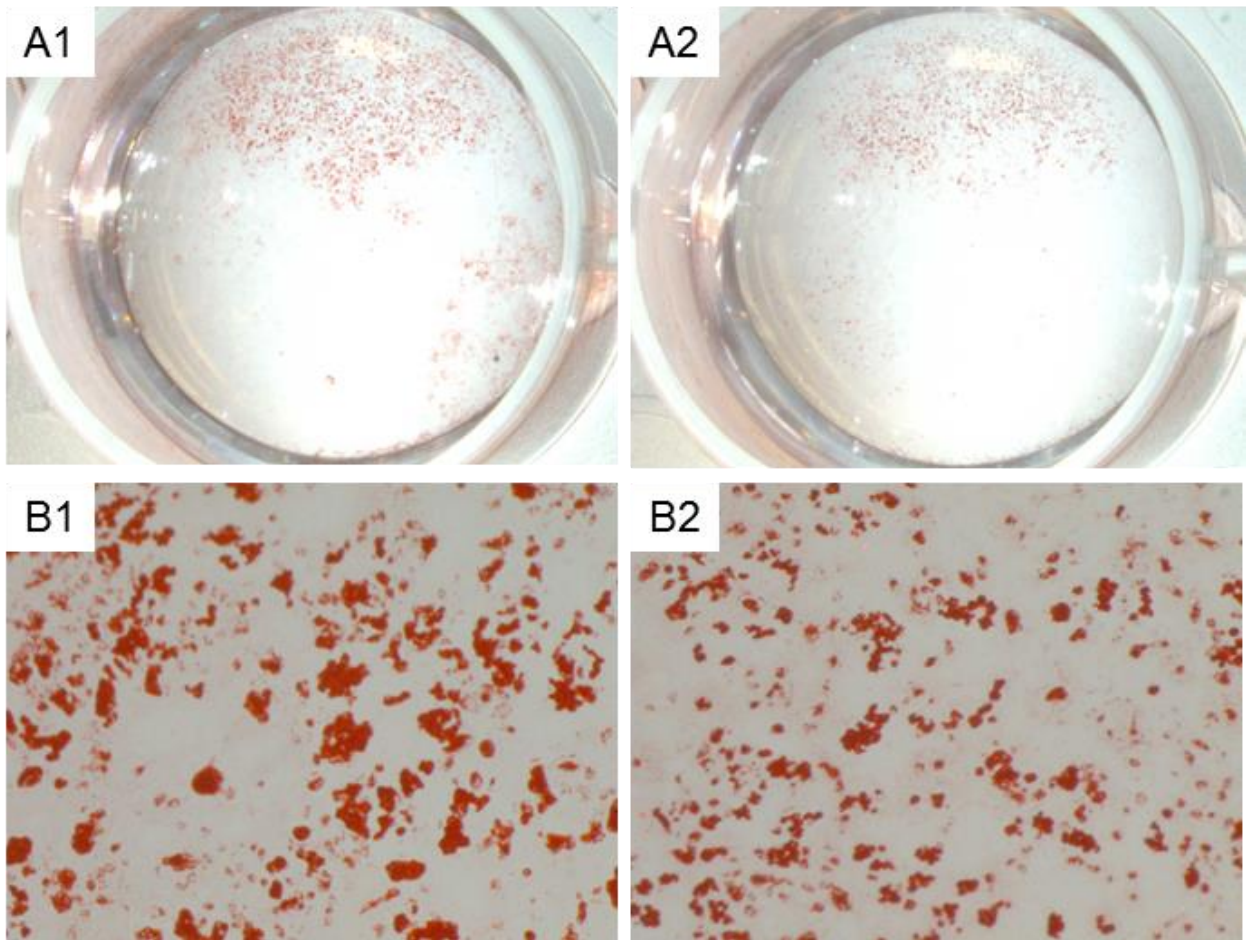


**Figure 28: Oil Red O staining of CD1 wt and mat E2KO ADSCs on Day 7 of adipogenic differentiation. (experiment #32)**

(A1) CD1 wt, 1x amplification. (A2) Mat E2KO, 1x amplification.

(B1) CD1 wt, 10x amplification. (B2) Mat E2KO, 10x amplification.

Abbreviations: CD1 wt, CD1 wild-type; mat E2KO, maternal exon 2 knockout; ADSCs, adipose-derived stromal cells.

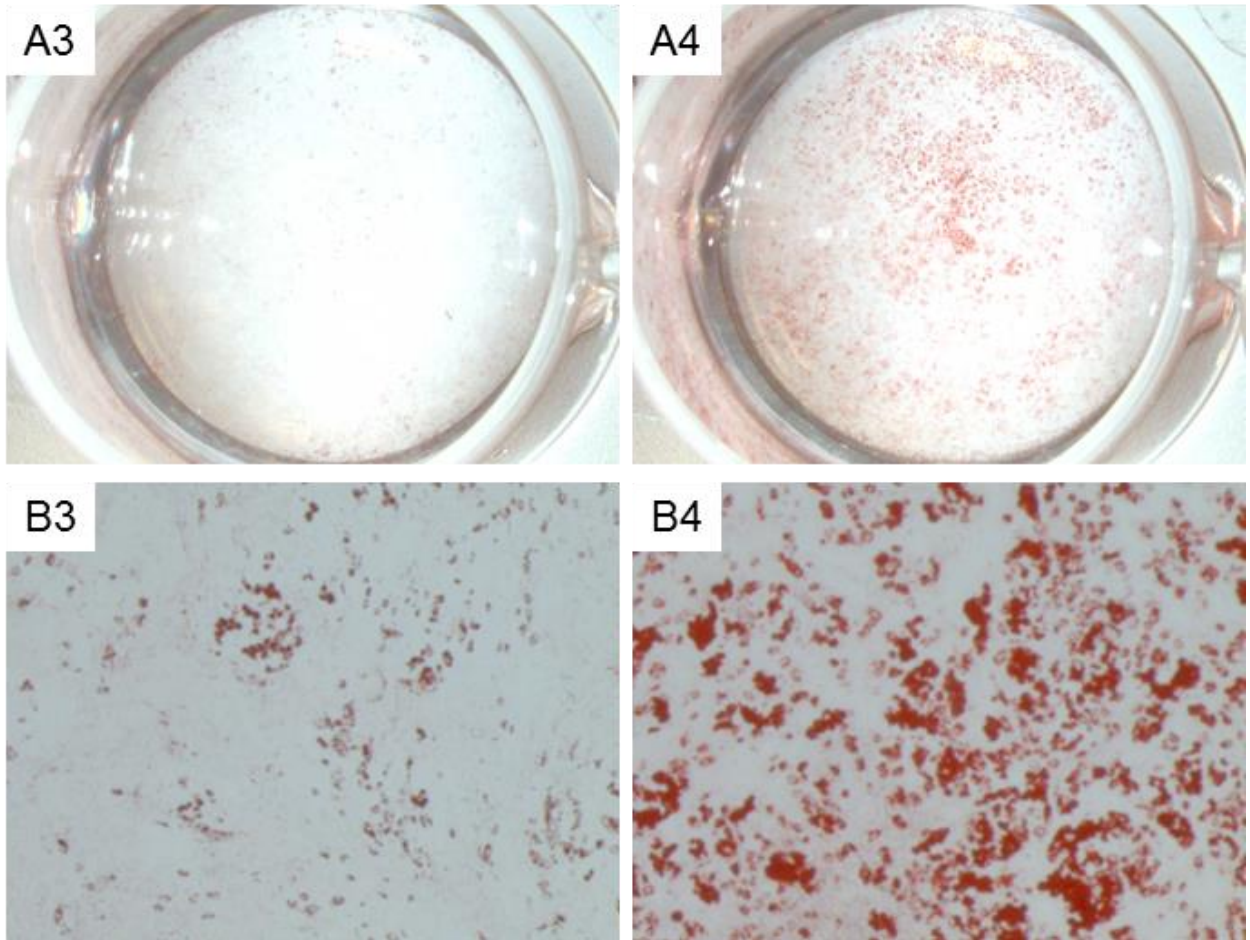


**Figure 29: Oil Red O staining of CD1 wt and mat E2KO ADSCs on Day 7 of adipogenic differentiation. (experiment #37)**

(A3) CD1 wt, 1x amplification. (A4) Mat E2KO, 1x amplification.

(B3) CD1 wt, 10x amplification. (B4) Mat E2KO, 10x amplification.

Abbreviations: CD1 wt, CD1 wild-type; mat E2KO, maternal exon 2 knockout; ADSCs, adipose-derived stromal cells.

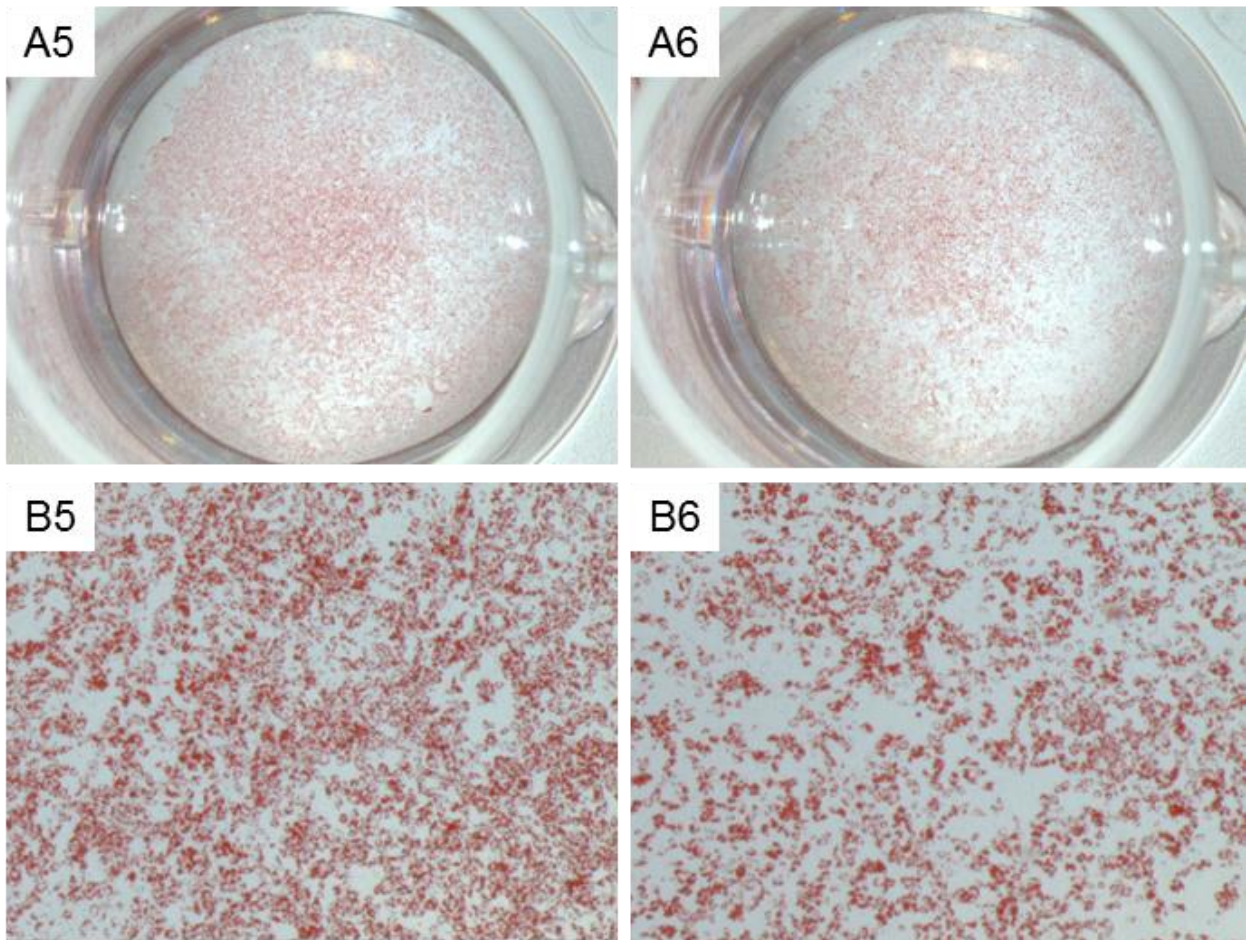


**Figure 30: Oil Red O staining of CD1 wt and mat E2KO ADSCs on Day 7 of adipogenic differentiation. (experiment #47)**

(A5) CD1 wt, 1x amplification. (A6) Mat E2KO, 1x amplification.

(B5) CD1 wt, 10x amplification. (B6) Mat E2KO, 10x amplification.

Abbreviations: CD1 wt, CD1 wild-type; mat E2KO, maternal exon 2 knock-out; ADSCs, adipose-derived stromal cells.



## 4 Discussion

Progressive osseous heteroplasia (POH) is a very rare bone disorder caused by heterozygous disruption in the *GNAS* allele on chromosome 20q13.2-13.3, which encodes the alpha-subunit of the stimulatory G protein (G $\alpha$ ). Inactivating mutations causing POH usually originate paternally. They elicit a progressive ossification that starts in subcutaneous fat tissue and advances to deep connective tissues, including skeletal muscle, tendons and ligaments. Further precise knowledge of signalling pathways is needed to better conceive the pathogenesis of this bone disease. Adipogenesis is regulated through several transcription factors. We investigated gene expression levels of the adipogenic markers peroxisome proliferator-activated receptor gamma (PPAR $\gamma$ ) and adipocyte lipid-binding protein (aP2) in adipose-derived stromal cells (ADSCs) during early differentiation to elucidate the activation pattern of these specific adipogenic genes. We chose ADSCs because ectopic ossification in patients with POH typically emanates from the subcutaneous tissue and osteogenesis may therefore involve abnormal lineage commitment of mesenchymal precursors that are present in this tissue. It has been shown that multipotential progenitor cells from adipose tissue can differentiate along an osteogenic and adipogenic lineage and that a reciprocal bipotential relationship between bone and fat cell differentiation may exist.<sup>65,104-106</sup> In this regard, it has further been shown that cAMP signalling has a pivotal impact, mediating opposing effects during early and late stages of osteogenic differentiation: cAMP signalling suppresses osteogenic differentiation during early stages, whereas increased levels of cAMP in late stages enhance osteogenic differentiation. Based on the reciprocal relationship between adipogenic and osteogenic differentiation, it has been also confirmed that increased levels of cAMP at early stages promoted adipogenesis, even under treatment with osteogenic induction factors.<sup>106</sup>

### **Parental origin of the mutant *GNAS* allele and its effects on the murine phenotype**

Another previous study by Yu et al. with *Gnas* exon 2 mice has shown that energy metabolism depends on the parent-of-origin of the disrupted allele.<sup>92</sup> In addition to a lean phenotype, knockout mice with a paternal deletion of the *Gnas* exon 2 allele presented with increased glucose tolerance, insulin sensitivity and sympathetic nervous system activity.<sup>44,91-93</sup> This lean phenotype, albeit much milder, could also be observed

in mice with paternally inherited *Gnas* exon 1 knockout mice<sup>65,72,90</sup>, suggesting that fat stores, in particular leanness, are regulated by the paternal allele expression of *GNAS* in humans.<sup>8,42,44,47,65,92</sup> *Gnasxl* knockout mice manifest a similar phenotype to paternal *Gnas* exon 2 knockout mice, sharing leanness with reduced lipid accumulation in adipose tissue.<sup>82,89</sup> In contrast, mice with a maternally inherited *Gnas* exon 2 knockout allele show, besides obesity with increased lipid accumulation in white and brown adipose tissue, increased serum leptin levels and decreased energy expenditure.<sup>44,92,93</sup>

### **Determination of allelic *Gsα* expression and additional screening for *XLαs* mRNA expression in the knockout mice**

Prior to analysing adipogenic marker expression in different knockout cells, we performed an investigation of expression levels of *Gsα* in undifferentiated (Day 0) ADSCs. This experiment not only served as a reference point for the successful targeted deletion of one copy of *Gsα* in the knockout mice, but also demonstrated that, unlike in certain tissues, such as brown adipose tissue and renal proximal tubules, *Gsα* expression in ADSCs is biallelic (Fig. 9 and Fig. 10). After isolation and successful proliferation of ADSCs, these cells were differentiated for 12 days, with an investigation of gene expression levels on Day 0, 3, 6 and 12 of differentiation. We also screened ADSCs from paternal and maternal E2KO mice for *XLαs* mRNA expression (Fig. 11 and Fig. 12). ADSCs isolated from paternal E2KO mice showed a markedly low expression of *XLαs* in comparison to CD1 wt ADSCs, which is consistent with the exclusively paternal transcription of *XLαs* (Fig. 11). A comparison of *XLαs* mRNA expression in ADSCs from maternal E2KO and CD1 wt mice shows about 40.1 % elevated *XLαs* mRNA expression in ADSCs from maternal E2KO mice, even though we expected similar *XLαs* expression in ADSCs from maternal E2KO and CD1 wt mice (Fig. 12). This finding could perhaps indicate a compensatory increase in *XLαs* expression in the face of reduced *Gsα* expression in an attempt to generate sufficient cAMP.

## **Adipogenic differentiation potential of ADSCs from paternal vs. maternal E2KO pups compared to ADSCs isolated from wild-type littermates**

In our experimental series, we compared absolute mRNA expression levels and mRNA expression levels normalized to CD1 wt Day 0 levels of PPAR $\gamma$  and aP2 in ADSCs from CD1 wt and paternal E2KO mice as well as in ADSCs from CD1 wt and maternal E2KO mice. Our gene expression experiments show two different trends, although the variation among experiments precludes us from making strong conclusions. Absolute values and data normalized to Day 0 levels of CD1 wt (figures with blue and green lines) exhibit an opposite trend with paternal E2KO cells differentiating more than wild-type and maternal E2KO cells showing seemingly normal adipogenic potential compared to wild-type. Induced adipogenic differentiation in our experiments could have been affected by how much adipogenic differentiation was already present at Day 0. The latter may depend on cell density and how much the cells had to be cultured before the induction of adipogenic conditions. ADSCs isolated from paternal E2KO mice tended to have elevated PPAR $\gamma$  and aP2 mRNA levels in comparison to wild-type cells before the initiation of adipogenic differentiation, i. e. on Day 0. Those cells showed little further differentiation into adipocytes compared to wild-type cells under adipogenic conditions (Fig. 13, Fig. 14, Fig. 15 and Fig. 16, respectively). This may be due to the fact that paternal E2KO cells have already reached quite high adipogenic gene expression levels.

ADSCs from maternal E2KO, however, appeared to have similar levels of adipogenic marker expression compared to wild-type cells before the initiation of adipogenic differentiation. Wild-type cells showed elevation of aP2 mRNA expression levels under adipogenic conditions, but the trend did not seem to differ significantly from the trend observed in maternal E2KO cells (Fig. 19 and Fig. 20, respectively). Regarding PPAR $\gamma$  mRNA expression levels, an increase of this marker was detected for maternal E2KO cells on Day 3 of differentiation (Fig. 17 and Fig. 18, respectively).

We expected similar PPAR $\gamma$  and aP2 mRNA expression levels as well as equal differentiation profiles in wild-type ADSCs in both paternal and maternal E2KO experiments. However, a comparison of absolute PPAR $\gamma$  and aP2 mRNA expression levels in ADSCs from CD1 wt mice between the two main experimental set-ups, i. e. paternal E2KO vs. CD1 wt and maternal E2KO vs. CD1 wt, showed a tendency toward higher expression of both markers in ADSCs from CD1 wt mice used in the maternal

E2KO experiments than in the paternal E2KO experiments (Fig. 21 and Fig. 22, respectively).

Since the differences were not statistically significant, this discrepancy may simply represent normal experimental variation. Alternatively, the differences between these experimental settings may suggest a possible influence of the genotype of the mother. The mothers used to generate paternal E2KO pups were wild-type females. In contrast, the mothers used to generate the maternal E2KO pups were paternal E2KO females (maternal E2KO mothers were not used due to their hormone resistance phenotype, such as hypocalcemia). Thus, it is conceivable that the gene expression profile is altered in the offspring of paternal E2KO females (even the wild-type offspring) during pregnancy and immediately after birth owing to an as-yet-unknown phenotype of the mother that likely results from *Gsa* haploinsufficiency.

Oil Red O stains of the cells following seven days of growth under adipogenic conditions did not reveal statistically significant differences. However, the mean levels tended to be higher in paternal E2KO ADSCs than wild-type ADSCs (Fig. 23), while they appeared to be similar in maternal E2KO ADSCs and wild-type ADSCs (Fig. 27). These observations are consistent with the general trend obtained from our gene expression experiments, particularly when data are analysed by normalizing to the values obtained from CD1 wild-type ADSCs at Day 0.

### **Opposing findings by Liu et al. and methodical differences compared to our study**

In contrast to our findings, a recent study by Liu et al. examining adipose-derived stromal cells from paternally inherited *Gsa*-specific exon 1 knockout mice and their capacity for adipogenic differentiation has shown an inhibition of adipogenesis compared to ADSCs from wild-type littermates. Moreover, in spite of adipogenic conditions, enhanced osteogenic differentiation could be observed in ADSCs with a paternally inherited deletion of *Gnas* exon 1.<sup>65</sup> Unexpectedly, ADSCs from *Gsa*-specific exon 1 knockout mice expressed reduced levels of XLAs, suggesting that the lineage commitment may be a combined effect of *Gsa* and XLAs.<sup>65</sup>

As opposed to our research method, ADSCs were not isolated from newborn mice, but from 3-month old adult mice. Furthermore, cells were isolated exclusively from male mice, whereas we pooled together ADSCs from newborn mice with same genotypical background, regardless of their sex. More importantly, Liu et al. used *Gsa*-specific exon 1 knockout mice, while we investigated exon 2 knockout mice, which lack XLAs entirely.

Unlike our research group, Liu et al. also used triiodo-L-thyronine (T3) in their differentiation media.<sup>65</sup>

In addition, studies by Pignolo et al. previously additionally revealed an enhanced expression of osteogenic markers, including alkaline phosphatase, osteopontin and osteocalcin, in *Gsα*-specific exon 1 knockout-derived adipocyte soft tissue stromal cells under osteogenic conditions in comparison to the same cells isolated from wild-type mice.<sup>104</sup> Moreover, our observations are not consistent with the phenotype of paternal and maternal E2KO mice, which are thinner with reduced lipid accumulation in white and brown adipose tissue<sup>44,91-93</sup>, or show an increased corporal mass of fat, respectively<sup>42,44,92,93</sup>. The *in vivo* phenotypes of those mice, however, can be explained by systemic factors. The paternal and maternal E2KO mice are hyper- or, hypometabolic and in addition, they show increased or decreased central sympathetic nervous system activity, respectively.<sup>92</sup> These differences in metabolism could override the cell-autonomous defects in adipogenic differentiation of ADSCs.

In summary, our investigation of ADSCs and their genotype-specific capacity for adipogenic differentiation could show mildly enhanced adipogenic potential for ADSCs from paternal E2KO mice and seemingly normal adipogenic potential for maternal E2KO mice compared to their wild-type littermates.

Initially, we hypothesized that XLAs deficiency combined with *Gsα* haploinsufficiency (as in paternal E2KO mice) impairs adipogenic lineage commitment of mesenchymal cells more readily than *Gsα* haploinsufficiency alone by further lowering the cAMP levels that are already reduced as a result of *Gsα* haploinsufficiency. As a consequence, we presumed that mesenchymal cells undergo osteogenesis more readily, thus contributing to the pathogenesis of POH.

Our findings are opposite of what we originally hypothesized, suggesting that XLAs deficiency in ADSCs increases their adipogenic differentiation potential. Therefore, we cannot confirm our hypotheses. However, as indicated above, because observed differences in adipogenic marker expression levels did not reach statistical significance, we cannot conclude whether these changes occurred by chance or they actually represent actual trends.

## **Variability of the experimental results**

The experiments led to quite variable results. In the paternal experiments, there is no common trend for both adipogenic markers. Whereas PPAR $\gamma$  mRNA expression levels in ADSCs from paternal E2KO mice increase until Day 3 of differentiation and thereafter gradually decrease, PPAR $\gamma$  mRNA expression levels in wild-type ADSCs rise until Day 6 of differentiation and decrease on Day 12 of differentiation. On the other hand, aP2 mRNA expression levels in ADSCs from paternal E2KO mice are generally higher compared to their wild-type littermates throughout the whole differentiation period with peaks on Day 3 and Day 6 of differentiation. A comparison with the corresponding aP2 mRNA expression levels in wild-type ADSCs shows an increase of aP2 mRNA expression on Day 3 that continues to grow to peak expression levels on Day 12 of differentiation.

Despite the overall variation, there is a more common trend in the maternal experiments: Both adipogenic markers, PPAR $\gamma$  and aP2, show a stable genotype-independent trend and similar mRNA expression levels with only minor differences in ADSCs from CD1 wt and maternal E2KO mice as compared to the more random course of the adipogenic mRNA expression curves in the paternal E2KO experiments. PPAR $\gamma$  and aP2 have peak expression levels on Day 3 and thereafter gradually decrease. Furthermore, both adipogenic marker expression levels are much higher in the maternal experimental set-up as compared to the paternal experimental set-up. These observations may all argue for a more successful induction of adipogenic differentiation in maternal E2KO experiments than paternal experiments.

As our data are quite variable among experiments, it is important to have a look at possible sources of error. This variability of gene expression levels may have different reasons and it seems as if cell systems of ADSCs are very sensitive in general and tend to be variable. On one hand, factors being different from one experiment to another could account for the contradictory gene expression levels. These include the initial seeding cell density for proliferation purposes after isolation, but also the time the cells were cultured before seeding for the differentiation experiment. Both may lead to premature differentiation in some cases, for example if cells get over-confluent and crowded, and this premature differentiation would prevent further differentiation under adipogenic conditions, thus distorting the results. For instance, Liu et al. have seeded 20,000 cells per cm<sup>2</sup>, which is the area for a 48-well plate, as opposed to our range of

35,000 to 50,000 cells per well.<sup>65</sup> In addition, mice were in the CD1 background, which is an outbred strain and may therefore additionally contribute to the variability. We deliberately kept the mice in CD1 background, because studies by Yu et al. showed that these knockout mice had better survival in this genetic background than in some of the pure backgrounds, in which no knockout mice indeed survived beyond weaning.<sup>44</sup>

From a more general point of view, other environmental factors, such as the non-standardized media with differentiation factors, that was prepared each time freshly for a media change, may account for premature or delayed differentiation. In addition, the adipogenic media that we used was based on  $\alpha$ MEM, following established protocols of our laboratory. In contrast, other research groups have used adipogenic media based on DMEM.<sup>65,111</sup> This different component of adipogenic media may cause adipogenic fate of cells less or more vigorously.

Furthermore, a fluctuation in the incubation temperature of the cells may cause variation among experiments, too. In addition, any further subsequent methodical proceeding of the cells or the cell RNA / cDNA harbours potential sources of error.

### **Research perspective**

A quantitation of osteogenic gene expression levels may be useful to further characterize the bipotential osteogenic-adipogenic lineage fate. In fact, these experiments have been started and are similar to the osteogenic differentiation experiments of ADSCs from mice with paternally inherited  $Gs\alpha$ -specific exon 1 disruption conducted by Pignolo et al.<sup>104</sup> Adipose-derived stromal cells in this case were cultured under osteogenic conditions to allow new insights into the osteogenic lineage commitment of these cells dependent on the genetic background. Pignolo et al. have shown that ADSCs from paternal *Gnas* exon 1 knockout mouse expressed osteogenic markers at higher levels even when the cells were differentiated in the presence of osteogenic media, indicating that paternally inherited  $Gs\alpha$  inactivating mutation potentiates osteogenic differentiation of stromal cells.<sup>104</sup>

In addition, one could expand, in this case, a quantitation of certain gene expression levels by flow cytometry, detecting early cells committed to adipogenic or osteoblastic lineage. For this purpose, transgenic mice in which green fluorescent protein (GFP) expression is driven for instance by the osterix promoter, an early osteoblastic

marker<sup>112</sup>, would need to be crossed with the relevant knockout mice prior to isolation of mesenchymal cells from mouse litters. If significant differences in knockout and wild-type mice can be shown, then in vitro-expanded multipotent cells can further be differentiated in vivo. For this purpose, one could transplant these cells under the skin of immunodeficient nude mice<sup>113,114</sup> and observe the formation of bone in real time at different time points. This has been previously performed with progenitor cells.<sup>115</sup> Likewise, an investigation of embryonic stem cells may be fruitful, especially with regard to osteoblast differentiation.<sup>116</sup>

A growing number of scientific investigations indicate that Gs $\alpha$  plays an important role in regulating the balance between osteogenesis and adipogenesis.<sup>65-67</sup> cAMP signalling has been shown to have a suppressive effect on osteogenic lineage recruitment of progenitor cells and is additionally associated with adipogenesis by induction of adipogenic transcriptional factors, such as PPAR $\gamma$ .<sup>65,107,108</sup>

Liu et al. demonstrated impaired adipocyte differentiation in ADSCs from paternal Gs $\alpha$ -specific exon 1 knockout mice which could be rescued by treatment with forskolin, an adenylyl cyclase activator, indicating that Gs $\alpha$ -cAMP signalling may be necessary in early adipogenesis.<sup>65</sup> In a different study, it has been shown that adipose stromal cells from paternally inherited Gs $\alpha$ -specific exon 1 knockout mice undergo an accelerated osteoblast differentiation under osteogenic conditions as compared to the same cells isolated from wild-type mice.<sup>104</sup>

## **Conclusion**

In conclusion, our investigation of ADSCs and their genotype-specific capacity for adipogenic differentiation can show mildly increased adipogenic potential for ADSCs from paternal E2KO mice and no significant difference in adipogenic potential for maternal E2KO mice compared to their wild-type littermates. There is growing evidence that a bipotential relationship between osteogenic and adipogenic cell fate may exist, and that *GNAS* inactivating mutations may direct cells into either of the two lineages depending on the parent-of-origin of the inherited disrupted allele. Thus, *GNAS* and, subsequently, the cAMP signalling may have a critical role in the regulation of cell fate decisions.

Assiduous subsequent studies involving, in particular, a third mouse model, i. e. XLas knockout mice, as well as investigating the osteogenic differentiation of ADSCs and



other cells in *Gnas* exon 2 knockout mice, as well as other novel genetically manipulated mice that are relevant to the *GNAS* locus, are crucial and indispensable in order to enhance our understanding of the regulation of *GNAS*, which in turn will help to further elucidate the pathogenesis of progressive osseous heteroplasia. From a more general point of view, new findings with respect to involved genes and signalling pathways can further contribute to the comprehension of cell-fate decisions and the overall regulation of heterotopic ossification.

As a complex and challenging disorder, new insights and a better understanding of the pathogenesis underlying POH may bring about change to prevent, diagnose, and treat people with other rare or more common diseases, for instance by potentially identifying new signalling molecules involved in the pathogenesis of POH. Recently, a study showed that most individuals with this disorder had a lesional bias toward one side or the other, and that the lesions had a dermomyotomal distribution, suggesting that this disease may stem from postzygotic defects that occur in addition to inherited heterozygous *GNAS* mutations.<sup>117</sup> A separate study has shown that complete loss of *Gsα* in the subcutis can also lead to ectopic ossifications that are similar to those found in POH patients.<sup>118</sup> Taken together, it is possible that the intact *Gnas* allele or another gene in the same pathway is also mutated in a postzygotic manner. Furthermore, the latter study indicated that the hedgehog signalling was elevated in POH lesions, further providing insights into the underlying mechanisms.

I would like to end my medical thesis with a quotation by William Harvey (1657), the discoverer of the systemic circulation of the blood (as cited by Kaplan and Shore<sup>6</sup>):

*"Nature is nowhere accustomed more openly to display her secret mysteries than in cases where she shows traces of her workings apart from the beaten path, nor is there any better method to advance the proper practice of medicine than to give our minds to the discovery of the usual law of nature by careful investigation of cases of rarer forms of disease."*<sup>119</sup>

## 5 Bibliography

1. Aymé S., Rodwell C., eds., "2012 Report on the State of the Art of Rare Disease Activities in Europe of the European Union Committee of Experts on Rare Diseases", July 2012.
2. Rare diseases / Public health / European Commission. (Accessed 7 September 2012, at [http://ec.europa.eu/health/rare\\_diseases/policy/index\\_en.htm](http://ec.europa.eu/health/rare_diseases/policy/index_en.htm).)
3. European Medicines Agency / Special Topics / Medicines for rare diseases. (Accessed 12 September 2012, at [http://www.ema.europa.eu/ema/index.jsp?curl=pages/special\\_topics/general/general\\_content\\_000034.jsp&mid=WC0b01ac058002d4eb](http://www.ema.europa.eu/ema/index.jsp?curl=pages/special_topics/general/general_content_000034.jsp&mid=WC0b01ac058002d4eb).)
4. Bulletin of the World Health Organization, Volume 90, Number 6, June 2012, 401-476.
5. Kaplan FS, Craver R, MacEwen GD, et al. Progressive osseous heteroplasia: a distinct developmental disorder of heterotopic ossification. Two new case reports and follow-up of three previously reported cases. *J Bone Joint Surg Am* 1994;76:425-36.
6. Kaplan FS, Shore EM. Progressive osseous heteroplasia. *J Bone Miner Res* 2000;15:2084-94.
7. Shore EM, Ahn J, Jan de Beur S, et al. Paternally inherited inactivating mutations of the GNAS1 gene in progressive osseous heteroplasia. *N Engl J Med* 2002;346:99-106.
8. Adegbite NS, Xu M, Kaplan FS, Shore EM, Pignolo RJ. Diagnostic and mutational spectrum of progressive osseous heteroplasia (POH) and other forms of GNAS-based heterotopic ossification. *Am J Med Genet A* 2008;146A:1788-96.
9. Shore EM, Kaplan FS. Inherited human diseases of heterotopic bone formation. *Nat Rev Rheumatol* 2010;6:518-27.
10. Karsenty G. The complexities of skeletal biology. *Nature* 2003;423:316-8.
11. Chan I, Hamada T, Hardman C, McGrath JA, Child FJ. Progressive osseous heteroplasia resulting from a new mutation in the GNAS1 gene. *Clin Exp Dermatol* 2004;29:77-80.
12. Kronenberg HM. Developmental regulation of the growth plate. *Nature* 2003;423:332-6.
13. Kaplan FS, Strear CM, Zasloff MA. Radiographic and scintigraphic features of modeling and remodeling in the heterotopic skeleton of patients who have fibrodysplasia ossificans progressiva. *Clin Orthop Relat Res* 1994:238-47.
14. Pignolo RJ, Shore EM, Kaplan FS. Fibrodysplasia ossificans progressiva: clinical and genetic aspects. *Orphanet J Rare Dis* 2011;6:80.
15. Schimmel RJ, Pasmans SG, Xu M, et al. GNAS-associated disorders of cutaneous ossification: two different clinical presentations. *Bone* 2010;46:868-72.
16. Eddy MC, Jan De Beur SM, Yandow SM, et al. Deficiency of the alpha-subunit of the stimulatory G protein and severe extraskeletal ossification. *J Bone Miner Res* 2000;15:2074-83.
17. Gelfand IM, Hub RS, Shore EM, Kaplan FS, Dimeglio LA. Progressive osseous heteroplasia-like heterotopic ossification in a male infant with pseudohypoparathyroidism type Ia: a case report. *Bone* 2007;40:1425-8.
18. Shore EM, Kaplan FS. Insights from a rare genetic disorder of extra-skeletal bone formation, fibrodysplasia ossificans progressiva (FOP). *Bone* 2008;43:427-33.
19. Geneviève D, Sanlaville D, Faivre L, et al. Paternal deletion of the GNAS imprinted locus (including Gnasxl) in two girls presenting with severe pre- and post-natal growth retardation and intractable feeding difficulties. *Eur J Hum Genet* 2005;13:1033-9.
20. Urtizbera JA, Testart H, Cartault F, Boccon-Gibod L, Le Merrer M, Kaplan FS. Progressive osseous heteroplasia. Report of a family. *J Bone Joint Surg Br* 1998;80:768-71.
21. Rodriguez-Jurado R, Gonzalez-Crussi F, Poznanski AK. Progressive osseous heteroplasia, uncommon cause of soft tissue ossification: a case report and review of the literature. *Pediatr Pathol Lab Med* 1995;15:813-27.

22. Kitterman JA, Strober JB, Kan L, et al. Neurological symptoms in individuals with fibrodysplasia ossificans progressiva. *J Neurol* 2012;259:2636-43.
23. Shore EM, Xu M, Feldman GJ, et al. A recurrent mutation in the BMP type I receptor ACVR1 causes inherited and sporadic fibrodysplasia ossificans progressiva. *Nat Genet* 2006;38:525-7.
24. Chakkalakal SA, Zhang D, Culbert AL, et al. An Acvr1 R206H knock-in mouse has fibrodysplasia ossificans progressiva. *J Bone Miner Res* 2012;27:1746-56.
25. Kaplan J, Kaplan FS, Shore EM. Restoration of normal BMP signaling levels and osteogenic differentiation in FOP mesenchymal progenitor cells by mutant allele-specific targeting. *Gene Ther* 2012;19:786-90.
26. Shen Q, Little SC, Xu M, et al. The fibrodysplasia ossificans progressiva R206H ACVR1 mutation activates BMP-independent chondrogenesis and zebrafish embryo ventralization. *J Clin Invest* 2009;119:3462-72.
27. Shore EM. Fibrodysplasia ossificans progressiva (FOP): A human genetic disorder of extra-skeletal bone formation, or - How does one tissue become another? *Wiley Interdiscip Rev Dev Biol* 2012;1:153-65.
28. Rocke DM, Zasloff M, Peeper J, Cohen RB, Kaplan FS. Age- and joint-specific risk of initial heterotopic ossification in patients who have fibrodysplasia ossificans progressiva. *Clin Orthop Relat Res* 1994:243-8.
29. Shafritz AB, Shore EM, Gannon FH, et al. Overexpression of an osteogenic morphogen in fibrodysplasia ossificans progressiva. *N Engl J Med* 1996;335:555-61.
30. Kaplan FS, Zasloff MA, Kitterman JA, Shore EM, Hong CC, Rocke DM. Early mortality and cardiorespiratory failure in patients with fibrodysplasia ossificans progressiva. *J Bone Joint Surg Am* 2010;92:686-91.
31. Kan L, Kitterman JA, Procissi D, et al. CNS demyelination in fibrodysplasia ossificans progressiva. *J Neurol* 2012;259:2644-55.
32. Lanchoney TF, Cohen RB, Rocke DM, Zasloff MA, Kaplan FS. Permanent heterotopic ossification at the injection site after diphtheria-tetanus-pertussis immunizations in children who have fibrodysplasia ossificans progressiva. *J Pediatr* 1995;126:762-4.
33. Mouallem M, Shaharabany M, Weintrob N, et al. Cognitive impairment is prevalent in pseudohypoparathyroidism type Ia, but not in pseudopseudohypoparathyroidism: possible cerebral imprinting of Gsalpha. *Clin Endocrinol (Oxf)* 2008;68:233-9.
34. Weinstein LS, Chen M, Xie T, Liu J. Genetic diseases associated with heterotrimeric G proteins. *Trends Pharmacol Sci* 2006;27:260-6.
35. Joseph AW, Shoemaker AH, Germain-Lee EL. Increased prevalence of carpal tunnel syndrome in albright hereditary osteodystrophy. *J Clin Endocrinol Metab* 2011;96:2065-73.
36. Yu D, Yu S, Schuster V, Kruse K, Clericuzio CL, Weinstein LS. Identification of two novel deletion mutations within the Gs alpha gene (GNAS1) in Albright hereditary osteodystrophy. *J Clin Endocrinol Metab* 1999;84:3254-9.
37. Rolla AR, Rodriguez-Gutierrez R. Images in clinical medicine. Albright's hereditary osteodystrophy. *N Engl J Med* 2012;367:2527.
38. Mantovani G, Elli FM, Spada A. GNAS epigenetic defects and pseudohypoparathyroidism: time for a new classification? *Horm Metab Res* 2012;44:716-23.
39. Bastepe M. Genetics and epigenetics of parathyroid hormone resistance. *Endocr Dev* 2013;24:11-24.
40. Clapham DE. Mutations in G protein-linked receptors: novel insights on disease. *Cell* 1993;75:1237-9.
41. Patten JL, Johns DR, Valle D, et al. Mutation in the gene encoding the stimulatory G protein of adenylate cyclase in Albright's hereditary osteodystrophy. *N Engl J Med* 1990;322:1412-9.
42. Weinstein LS, Yu S, Warner DR, Liu J. Endocrine manifestations of stimulatory G protein alpha-subunit mutations and the role of genomic imprinting. *Endocr Rev* 2001;22:675-705.

43. Levine MA. Pseudohypoparathyroidism: from bedside to bench and back. *J Bone Miner Res* 1999;14:1255-60.
44. Yu S, Yu D, Lee E, et al. Variable and tissue-specific hormone resistance in heterotrimeric Gs protein alpha-subunit (G $\alpha$ ) knockout mice is due to tissue-specific imprinting of the g $\alpha$  gene. *Proc Natl Acad Sci U S A* 1998;95:8715-20.
45. Mantovani G. Clinical review: Pseudohypoparathyroidism: diagnosis and treatment. *J Clin Endocrinol Metab* 2011;96:3020-30.
46. Davies SJ, Hughes HE. Imprinting in Albright's hereditary osteodystrophy. *J Med Genet* 1993;30:101-3.
47. Long DN, McGuire S, Levine MA, Weinstein LS, Germain-Lee EL. Body mass index differences in pseudohypoparathyroidism type 1a versus pseudopseudohypoparathyroidism may implicate paternal imprinting of G $\alpha$ (s) in the development of human obesity. *J Clin Endocrinol Metab* 2007;92:1073-9.
48. Kaplan FS. Skin and bones. *Arch Dermatol* 1996;132:815-8.
49. Hayward BE, Moran V, Strain L, Bonthron DT. Bidirectional imprinting of a single gene: GNAS1 encodes maternally, paternally, and biallelically derived proteins. *Proc Natl Acad Sci U S A* 1998;95:15475-80.
50. Hayward BE, Kamiya M, Strain L, et al. The human GNAS1 gene is imprinted and encodes distinct paternally and biallelically expressed G proteins. *Proc Natl Acad Sci U S A* 1998;95:10038-43.
51. Weinstein LS, Xie T, Qasem A, Wang J, Chen M. The role of GNAS and other imprinted genes in the development of obesity. *Int J Obes (Lond)* 2010;34:6-17.
52. Polychronakos C, Kukuvtis A. Parental genomic imprinting in endocrinopathies. *Eur J Endocrinol* 2002;147:561-9.
53. Reik W, Walter J. Genomic imprinting: parental influence on the genome. *Nat Rev Genet* 2001;2:21-32.
54. IZZI B, FRANCOIS I, LABARQUE V, et al. Methylation defect in imprinted genes detected in patients with an Albright's hereditary osteodystrophy like phenotype and platelet Gs hypofunction. *PLoS One* 2012;7:e38579.
55. Farfel Z, Bourne HR, Iiri T. The expanding spectrum of G protein diseases. *N Engl J Med* 1999;340:1012-20.
56. Bastepe M. Relative functions of G $\alpha$ s and its extra-large variant XL $\alpha$ s in the endocrine system. *Horm Metab Res* 2012;44:732-40.
57. Spiegel AM. Albright's hereditary osteodystrophy and defective G proteins. *N Engl J Med* 1990;322:1461-2.
58. Cabrera-Vera TM, Vanhauwe J, Thomas TO, et al. Insights into G protein structure, function, and regulation. *Endocr Rev* 2003;24:765-81.
59. Pasolli HA, Klemke M, Kehlenbach RH, Wang Y, Huttner WB. Characterization of the extra-large G protein alpha-subunit XL $\alpha$ s. I. Tissue distribution and subcellular localization. *J Biol Chem* 2000;275:33622-32.
60. Kozasa T, Itoh H, Tsukamoto T, Kaziro Y. Isolation and characterization of the human Gs alpha gene. *Proc Natl Acad Sci U S A* 1988;85:2081-5.
61. Gejman PV, Weinstein LS, Martinez M, et al. Genetic mapping of the Gs-alpha subunit gene (GNAS1) to the distal long arm of chromosome 20 using a polymorphism detected by denaturing gradient gel electrophoresis. *Genomics* 1991;9:782-3.
62. Weinstein LS, Xie T, Zhang QH, Chen M. Studies of the regulation and function of the Gs alpha gene Gnas using gene targeting technology. *Pharmacol Ther* 2007;115:271-91.
63. Bastepe M. The GNAS Locus: Quintessential Complex Gene Encoding G $\alpha$ , XL $\alpha$ s, and other Imprinted Transcripts. *Curr Genomics* 2007;8:398-414.
64. Wu JY, Aarnisalo P, Bastepe M, et al. G $\alpha$  enhances commitment of mesenchymal progenitors to the osteoblast lineage but restrains osteoblast differentiation in mice. *J Clin Invest* 2011;121:3492-504.

65. Liu JJ, Russell E, Zhang D, Kaplan FS, Pignolo RJ, Shore EM. Paternally inherited *gsa* mutation impairs adipogenesis and potentiates a lean phenotype in vivo. *Stem Cells* 2012;30:1477-85.
66. Nuttall ME, Patton AJ, Olivera DL, Nadeau DP, Gowen M. Human trabecular bone cells are able to express both osteoblastic and adipocytic phenotype: implications for osteopenic disorders. *J Bone Miner Res* 1998;13:371-82.
67. Sabatakos G, Sims NA, Chen J, et al. Overexpression of DeltaFosB transcription factor(s) increases bone formation and inhibits adipogenesis. *Nat Med* 2000;6:985-90.
68. Mantovani G, Bondioni S, Locatelli M, et al. Biallelic expression of the *Galpha* gene in human bone and adipose tissue. *J Clin Endocrinol Metab* 2004;89:6316-9.
69. Chen M, Wang J, Dickerson KE, et al. Central nervous system imprinting of the G protein G(s)alpha and its role in metabolic regulation. *Cell Metab* 2009;9:548-55.
70. Liu J, Erlichman B, Weinstein LS. The stimulatory G protein alpha-subunit *Gs alpha* is imprinted in human thyroid glands: implications for thyroid function in pseudohypoparathyroidism types 1A and 1B. *J Clin Endocrinol Metab* 2003;88:4336-41.
71. Germain-Lee EL, Ding CL, Deng Z, et al. Paternal imprinting of *Galpha(s)* in the human thyroid as the basis of TSH resistance in pseudohypoparathyroidism type 1a. *Biochem Biophys Res Commun* 2002;296:67-72.
72. Germain-Lee EL, Schwindinger W, Crane JL, et al. A mouse model of albright hereditary osteodystrophy generated by targeted disruption of exon 1 of the *Gnas* gene. *Endocrinology* 2005;146:4697-709.
73. Mantovani G, Ballare E, Giammona E, Beck-Peccoz P, Spada A. The *gsalpha* gene: predominant maternal origin of transcription in human thyroid gland and gonads. *J Clin Endocrinol Metab* 2002;87:4736-40.
74. Hayward BE, Barlier A, Korbonits M, et al. Imprinting of the *G(s)alpha* gene *GNAS1* in the pathogenesis of acromegaly. *J Clin Invest* 2001;107:R31-6.
75. Sakamoto A, Weinstein LS, Plagge A, Eckhaus M, Kelsey G. *GNAS* haploinsufficiency leads to subcutaneous tumor formation with collagen and elastin deposition and calcification. *Endocr Res* 2009;34:1-9.
76. Linglart A, Mahon MJ, Kerachian MA, et al. Coding *GNAS* mutations leading to hormone resistance impair in vitro agonist- and cholera toxin-induced adenosine cyclic 3',5'-monophosphate formation mediated by human *XLalphas*. *Endocrinology* 2006;147:2253-62.
77. Kehlenbach RH, Matthey J, Huttner WB. *XL alpha s* is a new type of G protein. *Nature* 1994;372:804-9.
78. Aydin C, Aytan N, Mahon MJ, et al. Extralarge *XL(alpha)s* (*XXL(alpha)s*), a variant of stimulatory G protein alpha-subunit (*Gs(alpha)*), is a distinct, membrane-anchored *GNAS* product that can mimic *Gs(alpha)*. *Endocrinology* 2009;150:3567-75.
79. Lebrun M, Richard N, Abeguilé G, et al. Progressive osseous heteroplasia: a model for the imprinting effects of *GNAS* inactivating mutations in humans. *J Clin Endocrinol Metab* 2010;95:3028-38.
80. Elli FM, deSanctis L, Ceoloni B, et al. Pseudohypoparathyroidism type 1a and pseudo-pseudohypoparathyroidism: the growing spectrum of *GNAS* inactivating mutations. *Hum Mutat* 2013;34:411-6.
81. Faust RA, Shore EM, Stevens CE, et al. Progressive osseous heteroplasia in the face of a child. *Am J Med Genet A* 2003;118A:71-5.
82. Plagge A, Gordon E, Dean W, et al. The imprinted signaling protein *XL alpha s* is required for postnatal adaptation to feeding. *Nat Genet* 2004;36:818-26.
83. Krechowec SO, Burton KL, Newlaczyl AU, Nunn N, Vlatković N, Plagge A. Postnatal changes in the expression pattern of the imprinted signalling protein *XLas* underlie the changing phenotype of deficient mice. *PLoS One* 2012;7:e29753.
84. Bastepe M, Weinstein LS, Ogata N, et al. Stimulatory G protein directly regulates hypertrophic differentiation of growth plate cartilage in vivo. *Proc Natl Acad Sci U S A* 2004;101:14794-9.

85. Michienzi S, Cherman N, Holmbeck K, et al. GNAS transcripts in skeletal progenitors: evidence for random asymmetric allelic expression of Gs alpha. *Hum Mol Genet* 2007;16:1921-30.
86. Klemke M, Pasolli HA, Kehlenbach RH, Offermanns S, Schultz G, Huttner WB. Characterization of the extra-large G protein alpha-subunit XLalphas. II. Signal transduction properties. *J Biol Chem* 2000;275:33633-40.
87. Liu Z, Segawa H, Aydin C, et al. Transgenic overexpression of the extra-large Gs $\alpha$  variant XL $\alpha$ s enhances Gs $\alpha$ -mediated responses in the mouse renal proximal tubule in vivo. *Endocrinology* 2011;152:1222-33.
88. Bastepe M, Gunes Y, Perez-Villamil B, Hunzelman J, Weinstein LS, Jüppner H. Receptor-mediated adenylyl cyclase activation through XLalpha(s), the extra-large variant of the stimulatory G protein alpha-subunit. *Mol Endocrinol* 2002;16:1912-9.
89. Xie T, Plagge A, Gavrilova O, et al. The alternative stimulatory G protein alpha-subunit XLalphas is a critical regulator of energy and glucose metabolism and sympathetic nerve activity in adult mice. *J Biol Chem* 2006;281:18989-99.
90. Chen M, Gavrilova O, Liu J, et al. Alternative Gnas gene products have opposite effects on glucose and lipid metabolism. *Proc Natl Acad Sci U S A* 2005;102:7386-91.
91. Chen M, Haluzik M, Wolf NJ, et al. Increased insulin sensitivity in paternal Gnas knockout mice is associated with increased lipid clearance. *Endocrinology* 2004;145:4094-102.
92. Yu S, Gavrilova O, Chen H, et al. Paternal versus maternal transmission of a stimulatory G-protein alpha subunit knockout produces opposite effects on energy metabolism. *J Clin Invest* 2000;105:615-23.
93. Yu S, Castle A, Chen M, Lee R, Takeda K, Weinstein LS. Increased insulin sensitivity in Gsalpha knockout mice. *J Biol Chem* 2001;276:19994-8.
94. Xie T, Chen M, Gavrilova O, Lai EW, Liu J, Weinstein LS. Severe obesity and insulin resistance due to deletion of the maternal Gsalpha allele is reversed by paternal deletion of the Gsalpha imprint control region. *Endocrinology* 2008;149:2443-50.
95. Liu J, Chen M, Deng C, et al. Identification of the control region for tissue-specific imprinting of the stimulatory G protein alpha-subunit. *Proc Natl Acad Sci U S A* 2005;102:5513-8.
96. Levine MA. An update on the clinical and molecular characteristics of pseudohypoparathyroidism. *Curr Opin Endocrinol Diabetes Obes* 2012;19:443-51.
97. Chen M, Berger A, Kablan A, Zhang J, Gavrilova O, Weinstein LS. Gs $\alpha$  deficiency in the paraventricular nucleus of the hypothalamus partially contributes to obesity associated with Gs $\alpha$  mutations. *Endocrinology* 2012;153:4256-65.
98. Ishikawa Y, Bianchi C, Nadal-Ginard B, Homcy CJ. Alternative promoter and 5' exon generate a novel Gs alpha mRNA. *J Biol Chem* 1990;265:8458-62.
99. Ischia R, Lovisetti-Scamihorn P, Hogue-Angeletti R, Wolkersdorfer M, Winkler H, Fischer-Colbrie R. Molecular cloning and characterization of NESP55, a novel chromogranin-like precursor of a peptide with 5-HT<sub>1B</sub> receptor antagonist activity. *J Biol Chem* 1997;272:11657-62.
100. Bastepe M. The GNAS locus and pseudohypoparathyroidism. *Adv Exp Med Biol* 2008;626:27-40.
101. Hayward BE, Bonthron DT. An imprinted antisense transcript at the human GNAS1 locus. *Hum Mol Genet* 2000;9:835-41.
102. Lietman SA, Ding C, Cooke DW, Levine MA. Reduction in Gsalpha induces osteogenic differentiation in human mesenchymal stem cells. *Clin Orthop Relat Res* 2005:231-8.
103. Weinstein LS, Shenker A, Gejman PV, Merino MJ, Friedman E, Spiegel AM. Activating mutations of the stimulatory G protein in the McCune-Albright syndrome. *N Engl J Med* 1991;325:1688-95.
104. Pignolo RJ, Xu M, Russell E, et al. Heterozygous inactivation of Gnas in adipose-derived mesenchymal progenitor cells enhances osteoblast differentiation and promotes heterotopic ossification. *J Bone Miner Res* 2011;26:2647-55.

105. Zuk PA, Zhu M, Ashjian P, et al. Human adipose tissue is a source of multipotent stem cells. *Mol Biol Cell* 2002;13:4279-95.
106. Zhang S, Kaplan FS, Shore EM. Different roles of GNAS and cAMP signaling during early and late stages of osteogenic differentiation. *Horm Metab Res* 2012;44:724-31.
107. Zhao Y, Ding S. A high-throughput siRNA library screen identifies osteogenic suppressors in human mesenchymal stem cells. *Proc Natl Acad Sci U S A* 2007;104:9673-8.
108. Tintut Y, Parhami F, Le V, Karsenty G, Demer LL. Inhibition of osteoblast-specific transcription factor Cbfa1 by the cAMP pathway in osteoblastic cells. Ubiquitin/proteasome-dependent regulation. *J Biol Chem* 1999;274:28875-9.
109. El-Ftesi S, Chang EI, Longaker MT, Gurtner GC. Aging and diabetes impair the neovascular potential of adipose-derived stromal cells. *Plast Reconstr Surg* 2009;123:475-85.
110. Maddox JR, Liao X, Li F, Niyibizi C. Effects of Culturing on the Stability of the Putative Murine Adipose Derived Stem Cells Markers. *Open Stem Cell J* 2009;1:54-61.
111. Wan DC, Shi YY, Nacamuli RP, Quarto N, Lyons KM, Longaker MT. Osteogenic differentiation of mouse adipose-derived adult stromal cells requires retinoic acid and bone morphogenetic protein receptor type IB signaling. *Proc Natl Acad Sci U S A* 2006;103:12335-40.
112. Nakashima K, Zhou X, Kunkel G, et al. The novel zinc finger-containing transcription factor osterix is required for osteoblast differentiation and bone formation. *Cell* 2002;108:17-29.
113. Bianco P, Kuznetsov SA, Riminucci M, Fisher LW, Spiegel AM, Robey PG. Reproduction of human fibrous dysplasia of bone in immunocompromised mice by transplanted mosaics of normal and Gsalpha-mutated skeletal progenitor cells. *J Clin Invest* 1998;101:1737-44.
114. Pettway GJ, Schneider A, Koh AJ, et al. Anabolic actions of PTH (1-34): use of a novel tissue engineering model to investigate temporal effects on bone. *Bone* 2005;36:959-70.
115. Lo Celso C, Fleming HE, Wu JW, et al. Live-animal tracking of individual haematopoietic stem/progenitor cells in their niche. *Nature* 2009;457:92-6.
116. Duplomb L, Dagouassat M, Jourdon P, Heymann D. Concise review: embryonic stem cells: a new tool to study osteoblast and osteoclast differentiation. *Stem Cells* 2007;25:544-52.
117. Cairns DM, Pignolo RJ, Uchimura T, et al. Somitic disruption of GNAS in chick embryos mimics progressive osseous heteroplasia. *J Clin Invest* 2013;123:3624-33.
118. Regard JB, Malhotra D, Gvozdenovic-Jeremic J, et al. Activation of Hedgehog signaling by loss of GNAS causes heterotopic ossification. *Nat Med* 2013;19:1505-12.
119. Garrod A. The lessons of rare maladies. *Lancet* 1928;1:1055-60.

## 6 Affidavit

"I, Sinan Akdeniz, certify under penalty of perjury by my own signature that I have submitted the thesis on the topic "Inactivating *Gnas*-mutations and their impact on the capacity of adipose-derived stromal cells to differentiate into adipocytes: Implications for the pathogenesis of progressive osseous heteroplasia". I wrote this thesis independently and without assistance from third parties, I used no other aids than the listed sources and resources.

All points based literally or in spirit on publications or presentations of other authors are, as such, in proper citations (see "uniform requirements for manuscripts (URM)" the ICMJE [www.icmje.org](http://www.icmje.org)) indicated. The sections on methodology (in particular practical work, laboratory requirements, statistical processing) and results (in particular images, graphics and tables) correspond to the URM (s.o) and are answered by me. My interest in any publications to this dissertation corresponds to those that are specified in the following joint declaration with the responsible person and supervisor. All publications resulting from this thesis and which I am author correspond to the URM (see above) and I am solely responsible.

The importance of this affidavit and the criminal consequences of a false affidavit (section 156,161 of the Criminal Code) are known to me and I understand the rights and responsibilities stated therein.

Date

Signature



## **7 Curriculum Vitae**

Mein Lebenslauf wird aus datenschutzrechtlichen Gründen in der elektronischen Version meiner Arbeit nicht veröffentlicht.

Mein Lebenslauf wird aus datenschutzrechtlichen Gründen in der elektronischen Version meiner Arbeit nicht veröffentlicht.

## 8 Acknowledgements

I would like to speak out my utmost gratitude and appreciation to my mentor and principal investigator Dr. Murat Bastepe. Thank you for your invitation to Boston. I felt honoured to be part of your research group. Your passion for research has been an exceptional and grand inspiration for me. Thank you for this wonderful and unique experience working with you!

My thanks go to Prof. Dr. Heiko Krude, who has supervised my doctoral promotion during my time in Berlin. Thank you for helpful discussions, your advice and assistance, always taking your time whenever I needed consultation.

I like to further thank Prof. Dr. Harald Jueppner for helpful discussions, Dr. Partha Sinha for protocol assistance and general experimental guidance, and Monica Reyes for her technical and administrative support. My thanks also go to the entire staff and researchers in the Endocrine Unit, making my time in Boston an enjoyable experience.

Finally, I like to sincerely thank the Hans Boeckler Foundation for financing this research stay and making this valuable experience come true for me.